SELF-ASSEMBLED MONOLAYERS AS PLATFORM FOR BIOSENSORS

Except where reference is made to the work of others, the work described in this thesis is my own or was done in collaboration with my advisory committee. This thesis does not include proprietary or classified information.

_____

Qin Wang

Certificate of Approval:

_____	_____
Vince Cammarata Associate Professor Chemistry	Curtis Shannon, Chair Professor Chemistry
_____	_____
Tung-Shi Huang Assistant Professor Food and Nutrition Science	Holly Ellis Assistant Professor Chemistry

_____

Stephen L. McFarland
Acting Dean
Graduate School

SELF-ASSEMBLED MONOLAYERS AS PLATFORM FOR BIOSENSORS

Qin Wang

A Thesis

Submitted to

the Graduate Faculty of

Auburn University

in Partial Fulfillment of the

Requirements for the

Degree of

Master of Science

Auburn, Alabama
December 16, 2005

SELF-ASSEMBLED MONOLAYERS AS PLATFORM FOR BIOSENSOR

Qin Wang

Permission is granted to Auburn University to make copies of this thesis at its discretion, upon request of individuals or institutions and at their expense. The author reserves all publication rights.

_____
Signature of Author

_____
Date of Graduation

VITA

Qin Wang was born on September 1, 1975 in Jingshan County, Hubei Province, China. She graduated from Jingshan High School in 1993. She attended East China University of Science and Technology for four years and graduated with a Bachelor of Science in chemistry in 1997. She then studied organic chemistry and worked as a research assistant at Shanghai Institute of Organic Chemistry, Chinese Academy of Sciences. She began her graduate studies in the Department of Chemistry at Auburn University in August 2000.

THESIS ABSTRACT

SELF-ASSEMBLED MONOLAYERS AS PLATFORM FOR BIOSENSORS

Qin Wang

Master of Science, December 16, 2005
(B.S., East China University of Science and Technology, 1997)

103 Typed Pages

Directed by Curtis Shannon

In chapter one, self-assembled monolayers (SAMs), the platform for biosensors, were discussed in detail regarding surface pK_a, stability, and chemical reactions. Mixed self-assembled monolayers, especially when incorporated with poly(ethylene)glycol, has become an important platform for protein immobilization as well as a model system for studying protein-surface interactions. Following self-assembled monolayers, the core technology of immunological biosensors, antibody immobilization, were discussed with emphasis on antibody orientation immobilization schemes. Last, a brief review of microscopy and characterization techniques used for biosensor research was given.

In chapter 2, random antibody immobilization on mixed SAMs of 16-mercaptohexadecanoic acid and 11-mercapto-1-undecanol formed at 60°C showed slightly higher surface antibody density than that formed at room temperature. Rabbit IgGs have been immobilized on uniform SAMs surface through Fc region attachment.

Non-contact mode AFM has been successfully used to image the attached antibody surface. It is speculated that antibodies on the surface adopt a parallel orientation. Further *in-situ* AFM antibody-antigen binding experiments in liquid need to be carried out to confirm the findings.

In chapter 3, rabbit anti-*Salmonella* IgGs were covalently immobilized on pure or mixed SAMs surfaces, and the antibody functionalized surfaces were capable of detecting *Salmonella enterica* Typhimurium in PBS solution. The surfaces of captured bacteria and bacteria coverage were examined by SEM. The random antibody immobilization approach provided highly uniform and partial surface bacteria coverage when exposed to high concentration of *Salmonella enterica* Typhimurium solution. Pure thioctic acid SAMs provided the best bacteria coverage of 7.83×10^6 cells/ cm^2 amongst all the SAMs tested. A preliminary study of the efficacy of site-directed antibody immobilization on detection of *Salmonella enterica* Typhimurium was carried out, and a bacteria density of 1.64×10^6 cells / cm^2 was achieved. Further optimization of the experimental conditions of site-directed method is needed in order to provide higher bacteria density on gold surfaces. The reported SAMs based protein immobilization provides a generic platform of bioreceptor immobilization in biosensor development which can be tailored for detection of *Salmonella enterica* Typhimurium and a variety of other foodborne pathogens.

ACKNOWLEDGEMENTS

The author would like to thank her research advisor, Dr. Curtis Shannon for his guidance and assistance during the entire course of the research. Thanks are extended to my committee members: Dr. Tung-Shi Huang, Dr. Vince Cammarata, Dr. Holly Ellis for their discussion and suggestions during the research project and the preparation of the manuscript. Appreciation is also given to all the faculty and staff in the chemistry department and members of the Shannon research group for their generous help during her graduate studies at Auburn University.

The author would also like to express her gratitude to her family, especially her mother, for their encouragement throughout the graduate program. In addition, the author would like to thank her friends: Yuming Chen, Xiaoguang Wang, Michael Richardson, Ann Wang and Prof. Peter Johnson for their support.

Style manual or journal used Analytical Chemistry

Computer software used Microsoft Office XP, ISIS / DRAW2.0, EndNote6.0, PSI Prosan1.0

TABLE OF CONTENTS

LIST OF FIGURES xi

LIST OF TABLES xiv

CHAPTER 1 INTRODUCTION TO BIOSENSORS, SELF-ASSEMBLED MONOLAYERS AND MICROSCOPY 1

1.1 Biosensors: definition 1

1.2 Biosensors: background 3

1.3 Self-assembled monolayers: a versatile platform for biosurface formulation 4

1.3.1 Definition, Preparation 6

1.3.2 Stability of SAMs 7

1.3.3 Reaction and reactivity of SAMs 8

1.3.4 Mixed SAMs 11

1.4 Immobilization of biological molecules and biosurface formulation methods 14

1.4.1 Physical adsorption 15

1.4.2 Covalent immobilization 16

1.5 Modern microscopy: tools for biosensor research 22

1.5.1 Optical microscopy and electron microscopy 23

1.5.2 Scanning probe microscopy (SPM) 24

1.6 Conclusion 28

1.7 References 30

CHAPTER 2 COVALENT IMMOBILIZATION OF ANTIBODIES ON SELF-ASSEMBLED MONOLAYER SURFACES AND CHARACTERIZATION WITH NON-CONTACT ATOMIC FORCE MICROSCOPY 36

2.1 Introduction 36

2.2 Experimental 39

2.3 Results and Discussion 41

2.4 Outlook and Conclusion 52

2.5 References 53

CHAPTER 3 CAPTURE ANTIBODIES IMMOBILIZED ON SELF-ASSEMBLED MONOLAYERS FOR *SALMONELLA enterica* TYPHIMURIUM DETECTION 58

3.1 Introduction 58

3.2 Experimental 61

3.3 Results and Discussion 64

3.4 Conclusion 84

3.5 Acknowledgement 85

3.6 References 86

LIST OF FIGURES

Figure 1.1 Schematic representation of a biosensor array system.....2

Figure 1.2 Number of papers published in English, organized by year in the field of biosensors.....5

Figure 1.3 Carboxylic acid end groups on SAMs react with EDC or EDC/NHS 12

Figure 1.4 Structure of a typical IgG molecule 17

Figure 2.1 Reaction scheme of Fc antibody immobilization on SAMs……43

Figure 2.2 Contact-mode AFM topographical image of bare Au(111) surface…….44

Figure 2.3 Contact-mode AFM topographical image of mixed SAMs…… …….46

Figure 2.4 NC AFM topographical image of randomly immobilized antibodies on SAMs 47

Figure 2.5 NC AFM topographical image of antibody immobilized through carbohydrate region on SAMs…….. 48

Figure 3.1 Control experiment: SEM image (500×) of captured *Salmonella enterica* Typhimurium on butanethiol SAMs. 67

Figure 3.2 Control experiment: SEM image (500×) of captured *Salmonella enterica* Typhimurium on butanethiol SAMs pretreated with anti-*Salmonella* antibody solution.....68

Figure 3.3 SEM image (500×, 176 μm) of captured *Salmonella enterica* Typhimurium on mixed SAMs. [TA]/[TA]+[BT] = 0.1 71

Figure 3.4 SEM image (500×) of captured *Salmonella enterica* Typhimurium on mixed SAMs. [TA]/[TA]+[BT] = 0.4 72

Figure 3.5 SEM image (500×) of captured *Salmonella enterica* Typhimurium on 3-mercaptopropanoic acid SAMs 73

Figure 3.6 SEM image (500×) of captured *Salmonella enterica* Typhimurium on pure thioctic acid SAMs 74

Figure 3.7 SEM image (500×) of captured *Salmonella enterica* Typhimurium on pure thioctic acid SAMs with overlay of a grid system shown for point counting 76

Figure 3.8 Number of captured *S. enterica* Typhimurium cells on surface as a function of surface thioctic acid concentration 77

Figure 3.9 SEM image (500×) of captured *Salmonella enterica* Typhimurium on mixed SAMs. [3-MPA]/[11-MUA]=10/1 79

Figure 3.10 SEM image (2000×) of captured *Salmonella enterica* Typhimurium on mixed SAMs. [3-MPA]/[11-MUA]=10/1 80

Figure 3.11 SEM image (120×) of captured *Salmonella enterica* Typhimurium on mixed SAMs. [3-MPA]/[11-MUA]=10/1 81

Figure 3.12 SEM image (500×) of captured *Salmonella enterica* Typhimurium on 11-amino-undecanethiol monolayers 83

LIST OF TABLES

Table 1.1 Comparison of bulk vs. SAMs $pK_{1/2}$ for functionalized alkanethiols 10

Table 1.2 Summary of microscopy for imaging biological samples 29

Table 2.1 Comparison of site-directed and random immobilization……...50

Table 3.1 *S. enterica* Typhimurium density on SAMs and SAMs composition……..69

CHAPTER 1 INTRODUCTION TO BIOSENSORS, SELF-ASSEMBLED MONOLAYERS AND MICROSCOPY

1.1 Biosensors: definition

There are three general categories of sensors and sensor applications.[1] First, remote sensing, that is, sensing systems that are a large distance from the source/environment. These are usually optical-based systems. Second category is the analytical instruments- spectroscopic and/or separation instruments that perform chemical analysis, such as GC, GC/MS, HPLC, FTIR, AES, etc. The third category is point sensing, i.e., a sensor/transducer or small array located directly in the environment at a single or a few points. The biosensors discussed in this review belong to the third category.

Biosensors are members of the chemical sensor families. A chemical sensor, by definition, is a self-contained analytical device that is capable of detecting chemical species quantitatively. A typical chemical sensor has three components: a sample recognition element, a signal transducing structure, and a processing and amplification element. For biosensors, the sample recognition element should be an element that is able to recognize biological species. Hence, biosensors are self-contained analytical devices that are characterized by having a biological sensing element intimately connected or integrated within transducers which convert biological events into responses that can be further processed.[2] A schematic diagram of a biosensor is shown in Figure 1.1.

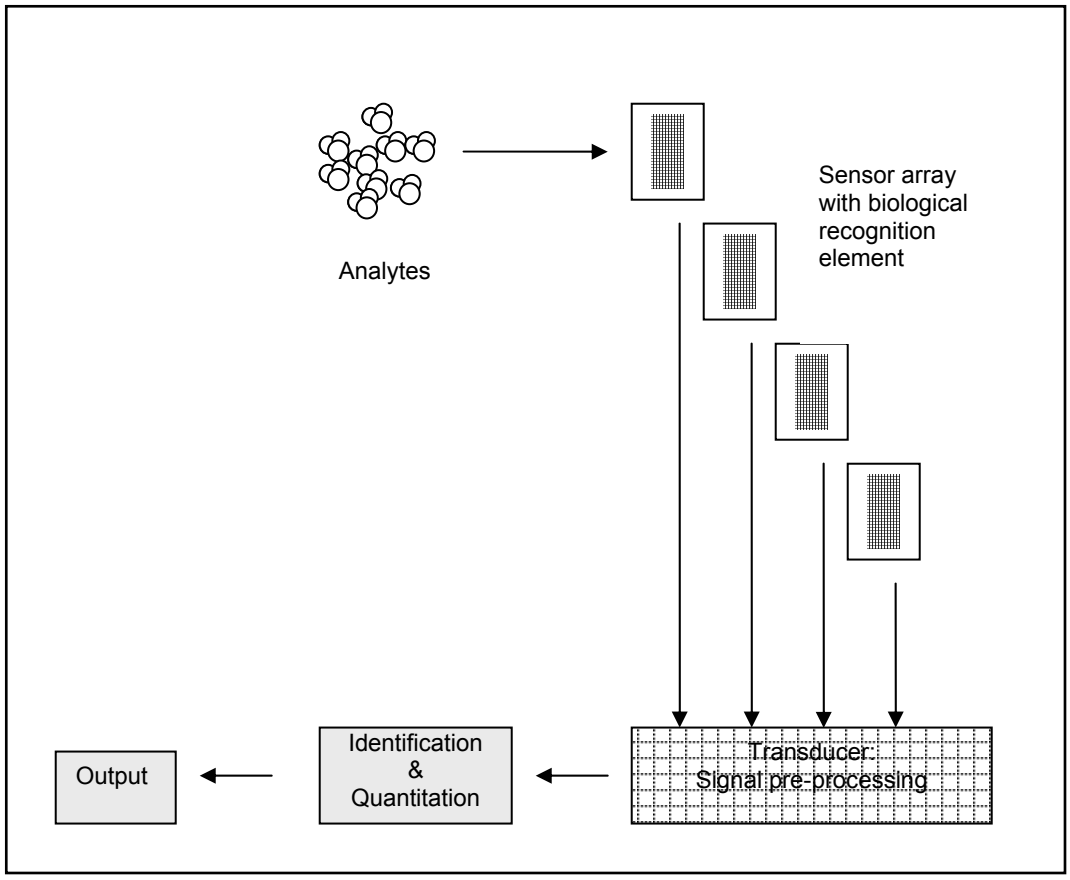

Figure 1.1 Schematic representation of a biosensor array system

1.2 Biosensors: background

Since the first biosensor was invented in 1962, the effort that has been put into biosensor research has grown exponentially over four decades. In 1962, Clark and Lyons[3] used glucose oxidase as the sensing element and an amperometric oxygen electrode as the transducer to detect glucose concentration. In 1967, Updike and Hicks[4] gave the name "enzyme electrode" to an oxygen electrode for detecting glucose which comprised a polyacrylamide gel with entrapped glucose oxidase coating the electrode. When this electrode is placed in contact with a solution that contains glucose and oxygen, which diffuse into the enzymatic membrane, glucose is oxidized into gluconic acid, while the oxygen electrode detects the reduction in oxygen partial pressure that is stoichiometric to the glucose concentration. This invention of the "enzyme electrode" was a landmark of biological sample analysis. Before this discovery, electrochemistry methods only detected anions and cations. When associated with biological systems such as enzymes, immunological agents, cells, microorganisms, the electrochemical sensors provided stable, fast detection to a wealth of other species, which otherwise could only be measured by laborious experimental methods. From this point forward, biosensors, a class of new sensors, were created.

The biological sensing element can be either catalytic, such as enzymes, or non-catalytic, such as antibodies. Catalytic biosensing elements rely on enzymes to liberate a product or consume a cosubstrate that is detected by a transducer. Non-catalytic biosensing element directly exploits a variation in parameters resulting from an immunological coupling.

The transducer, a system that transforms one physical quantity into another, usually falls into one of the following categories: electrochemical (amperometric, potentiometric), calorimetric, acoustic, or optical. Several reviews[5-9] on transducer platforms are available.

Biosensor construction usually involves combining the two basic elements, which includes three steps. A bioreceptor is chosen followed by a transducer, and finally, the biological component is fixed to the transducer.

Biosensor research and development has become one of the fastest growing fields. Figure 1.2 shows the number of papers published from 1996 to 2004 found by searching the research topic "biosensors" using ScifinderScholar.

1.3 Self-assembled monolayers: a versatile platform for biosurface formulation

Immobilization of the biological recognition element is of prime importance for biosensor construction. In the early development of biosensors, physical adsorption was employed to preserve the integrity of bioreceptors. Later, it was realized that covalent attachment would prevent bioreceptor loss and enhance biosensor stability. One of the most important properties of self-assembled monolayers, abbreviated as SAMs, is to generate a monolayer surface with functionality that is able to attach biological molecules for biosensor construction.

The conventional method of organic monolayer formation, i.e., Langmuir-Blodgett (LB) method,[10] is to spread an insoluble compound on an aqueous subphase, compress the top layer of thin film mechanically with barriers until the molecules in the layer are densely packed and oriented normal to the surface, then transfer the monolayer

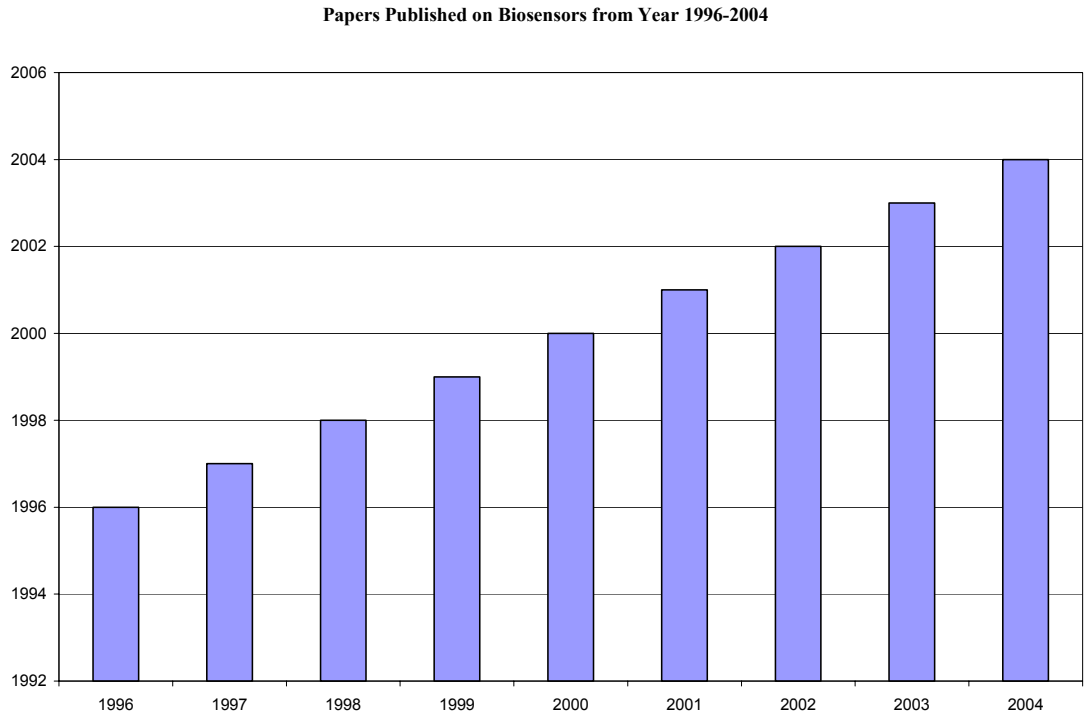

Figure 1.2 Number of papers, published in English, organized by year in the field of biosensors

to a solid support. Compared to the SAMs technique, the LB technique has some drawbacks when applied to form a biosurface. For example, LB monolayers are not thermally stable and are not chemically linked to a substrate, so the monolayers tend to change during the transfer process. The SAMs technique has demonstrated superiority over the LB technique during the past decade for biosurface formation.

There are a variety of SAMs systems made by chemical adsorption, such as alkylchlorosilanes with long alkyl chains on glass, silica or metal oxide and organosulfur compounds (thiols, disulfide, sulfides) on metals (gold, silver, platinum). In this review, the scope of SAMs is specifically referred to the organosulfur (organic thiols, sulfides and disulfides) monolayer formed on gold surface.

1.3.1 Definition, Preparation

Self-assembled monolayers (SAMs) are a single layer of highly ordered molecules of a surfactant formed spontaneously on a substrate when exposed to a surfactant solution. The procedure for preparation of SAMs on gold is simple: immerse the substrate in a 1-10 mM alkanethiol solution at room temperature for 24 hours. The resulting monolayer is an extremely dense-packed, crystalline monolayer. The surface density of thiols on the gold substrate is ca. 4×10^{14} molecules/cm^2.

Since the discovery of SAMs, the SAMs technique has been widely used in wetting,[11-13] adhesion,[14-16] corrosion,[17-20] catalysis,[21, 22] nanolithography[23-27] and biosensors.[28-30] The popularity of thiols on gold SAMs can be attributed to several reasons. First, the SAMs formation and preparation is simple, reliable and reproducible. Second, it is easy to control the surface density of the functional groups and molecular

environment. Third, it is very flexible to generate a wide variety of biosurfaces when SAMs are chosen as the platform.

1.3.2 Stability of SAMs

The thermal stability and chemical reactivity of self-assembled monolayers are essential to determine the range of applications, such as biosurface formation. According to contact angle, ellipsometry and FT-IR studies, SAMs of thiols on gold are very stable at room temperature in air and water. However, immersion of thiol SAMs in organic solvents showed desorption.[31]

Similar desorption was observed for immersed monolayers in solvents at elevated temperatures, according to thickness measurements.[31] It was observed that the desorption rates decreased in the order of organic solvents, water and air. However, when temperatures were above 80°C, thiol monolayers desorb rapidly in air. It was reported that when annealed in vacuum at 300°C, thiol monolayers were completely desorbed and only Au (111) surface were left. Annealing in air, according to XPS studies, oxidizes thiol monolayers on gold. The primary reason for the limited stability is the oxidation of sulphur head groups.[31]

The chemical stability of thiol SAMs also needs to be addressed when applied to chemical reactions and biosurface formation. Strong oxidizing reagents, such as peroxides, ozone, halogens (I_2, Br_2), and compounds that are capable of attacking gold surfaces, such as *aqua regia*, mercury, iodide and cyanide destroy thiol SAMs on gold. Studies[31] have also shown that monolayers of octadecanethiol on gold were unaffected by immersion in 1M NaOH or 1M HCl for 1 day. However, signs of deterioration were

evident after a month. Due to their different stabilities in contact with chemicals, caution is suggested when new reactions are conducted.

1.3.3 Reaction and reactivity of SAMs

1.3.3.1 Surface pK_a

SAMs with functional groups such as carboxyl, amino, hydroxyl or pyridine groups have been used to generate a wide variety of other functional groups through chemical modification. As the surface area to volume ratio of the surface-confined functional groups becomes larger, the dissociation of surface-confined functional groups and the specific adsorption of counter ions have become one of the important properties of SAMs, since they generate surface charges. The surface properties of self-assembled monolayers, such as wetting and adhesion, are also affected by the charged state.

In order to understand the surface charged state, it is important to understand the proton exchange abilities, i.e. the surface pK_a. At solid-liquid interfaces, the ability of the terminal group to exchange protons is different from the solvation process in the bulk media. This difference in pK_a has great impact on the surface selectivity and sensitivity. A number of techniques,[32-39] such as contact angle titration,[40] quartz crystal microbalance measurement[41] and chemical force measurement[42-44] have been applied to determine the surface pK_a.

Most of the calculations from these measurements are based on Henderson-Hasselbach equation:

$$pK_a = pH - \log ([A^-]/[HA])$$

When the acid or base is half-ionized, pK_a equals pH. For example, "contact angle titration" is a simple method that determines the acidity of surface. In this method, contact angles are measured for a series of buffered water droplets as a function of the pH of the droplet. Surface deprotonation usually changes the wetting properties of the surface. More ionized surfaces result in more hydrophilic surfaces. The function of contact angle vs. pH resembles a titration curve of acid or base in bulk media. In bulk media, pK_a can be determined from the midpoint of a titration curve, where the acid or base is half-ionized. By analogy to bulk media, surface $pK_{1/2}$ is defined as the pH where the surface is half-ionized according to the "contact angle titration curve". In this sense, pK_a and $pK_{1/2}$ are interchangeable.

Functional groups on the surface become less acidic or basic, usually 2~5 pK_a units different from that of bulk media. Table 1.1 is a list of surface pK_a and bulk pK_a of carboxylate and amine-terminated alkanethiols.

1.3.3.2 Chemical reactions in monolayers

Organic reactions on SAMs, such as nucleophilic substitution and oxidation/reduction reactions are similar to those in bulk. These reactions have important applications in biointerface formation of biosensors as well as DNA and protein microarray chips when combined with microcontact printing techniques (μCP). An excellent review on reactions and reactivity of SAMs by Chechik[47] can be found in the literature and will not be discussed in detail here. Mostly, the reactions on SAMs to form biosurfaces are conducted on monolayers with $-NH_2$, -COOH and -OH functional end groups.

Table 1.1 Comparison of bulk vs. SAMs $pK_{1/2}$ for functionalized alkanethiols

Thiol	Surface pKa	Bulk pKa	Reference
$HS(CH_2)_{15}COOH$	8.0	4.5	41
$HS(CH_2)_7COOH$	8.0	4.5	45
$HS(CH_2)_5COOH$	6.0	4.5	39
$HS(CH_2)_2COOH$	5.8	4.5	39
$HS(C_6H_4)COOH$	7.0	5.5	46
aminoethanethiol	5.0	10.5	33
6-amino-1-hexanethiol	3.8	10.5	33

Carboxylic acid as a functional end group usually needs to be activated before coupled to nucleophilic reagents. Usually the activation agent involves dicyclohexylcarbodiimide (DCC) or (1-Ethyl-(3-dimethylaminopropyl)carbodiimide) (EDC). EDC is a water-soluble coupling agent widely used in peptide synthesis. In the activation step (Figure 1.3), carbodiimide is protonated, and then the carboxylate attacks the C atom of the cation that was formed. This leads to the formation of the very active O-acylisourea.[48] The unstable intermediate O-acylisourea usually results in lower yield of the product amide. More often, a mixture of EDC and N-hydroxysuccinimide (NHS) are used. The resulting intermediate NHS esters are stable at neutral conditions and do not hydrolyze easily. After 3-4 cycles of EDC/NHS treatment, an 80% yield of amide can be achieved.[49]

A wide range of characterization techniques have been used to study the reactions on SAMs surface, including X-ray photoelectron spectroscopy (XPS), electrochemical methods, infrared spectroscopy (IR), ellipsometry, atomic force microscopy (AFM) and scanning tunneling microscopy (STM).

1.3.4 Mixed SAMs

When mixing two different organothiols, concentration gradients of the end groups can be controlled on SAMs. The end groups on SAMs have led to the formulation of a number of reactive surfaces for further derivatizations. By controlling concentration of functional groups on a SAMs surface, the concentration of protein attachment on the SAMs surface can be controlled. Since mixed SAMs have highly controllable structures

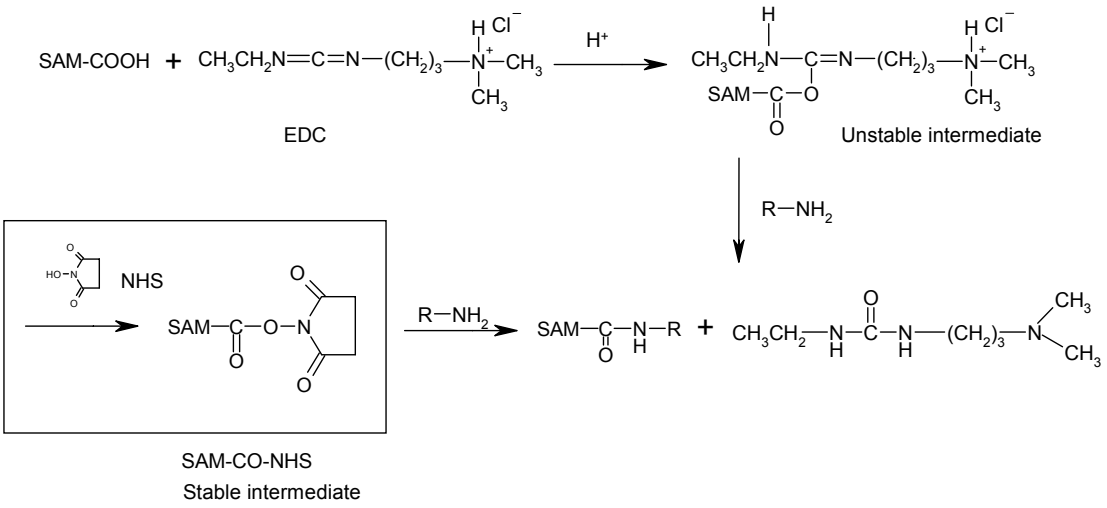

Figure 1.3 Carboxylic acid end groups on SAMs react with EDC or EDC/NHS

and properties of the surfaces, they have been widely used in generating biomolecular surfaces. In recent years, poly ethylene glycol (PEG)-terminated alkanethiols have been incorporated into mixed SAMs in a large percentage of the literature about mixed SAMs.

Mixed SAMs can be used as a model system for studying the adsorption of proteins to hydrophobic surfaces. The mixed self-assembled monolayers of two alkanethiolates $-S(CH_2)_{11}(OCH_2CH_2)_6OR$ and $-S(CH_2)_{11}(OCH_2CH_2)_nOH$, n=3, 6 in combination with surface plasmon resonance spectroscopy was used to study the influence of the size and shape of R, its density at the surface on the hydrophobic adsorption of proteins at solid-liquid interfaces. Detailed results were obtained for galactosidase, carbonic anhydrase, lysozyme, and RNase A when using different hydrophobic R groups.[50]

The monolayer thiolate composition is not necessarily the same as the thiolate composition of solution. Nelson, et al. prepared mixed SAMs by binary mixtures of a biotinylated alkylthiol (BAT) and either a C16 methyl-terminated thiol (mercaptohexadecane, MHD) or a C11-oligo(ethylene glycol)-terminated (OEG) thiol in ethanol[51] to immobilize streptavidin. There was a nonlinear relationship between the solution mole fraction of BAT and its surface mole fraction. The authors attributed the difference to the different rate constants for adsorption of the different thiols. The degree of specific binding of streptavidin to these surfaces was directly correlated with the amount of ligand (BAT) and the nature of the diluent thiol (MHD or OEG) and thus with the structure and physical properties of the SAMs.

Mixed SAMs consist of two different functionalities, which allows attachment of bioreceptor molecules and avoids nonspecific adsorption. Frederix[52] used mixed SAMs

of thiols with carboxylic and hydroxyl or poly- (ethylene glycol) groups to immobilize antibodies. Surface plasmon resonance measurements showed the enhanced performance of these mixed SAMs with regard to sensitivity, stability, and selectivity compared to commercially available affinity biosensor interfaces.

Mixed alkanethiol self-assembled monolayers also are used as substrates for microarray applications.[53] By altering the relative populations of methyl and hydroxyl groups, one can fine-tune the surface properties of alkanethiol SAM films to affect the size and amount of material transferred into the microarray spots.

1.4 Immobilization of biological molecules and biosurface formulation methods

Reactive functionality on SAMs has been used to covalently attach proteins onto SAM on solid support. The application has been used in developing biological sensors, as well as studying protein/surface and ligand/receptor interactions. The most important biological molecules to be immobilized on transducer surfaces are enzymes and antibodies. DNA and RNA immobilization on transducer surfaces is becoming important as well. Most of the immobilization techniques in today's literature derive from immunochemistry and affinity chromatography developed between the 1960's and 1980's. Since the emphasis of this thesis is on immunosensing, the focus of this review will be mainly on antibody immobilization. However, the techniques described here apply to other proteins as well.

A successful immobilization scheme requires: (1) reproducibility and stability of the antibody layer, (2) uniformity of the surface structures (3) the possibility to control the immobilization density of the immobilized species, (4) if possible, higher

coverage/density is preferred, and (5) orientation of antibodies so that maximum binding density can be achieved.

1.4.1 Physical adsorption

Antibodies adsorb to a variety of surfaces. Immobilization by passive adsorption works very well on some surfaces, such as polystyrene, although the mechanism has not been well understood. It is generally believed that the adsorption takes place due to hydrophobic, ionic, and Van der Waals interactions. Physical adsorption is the basis of assays such as EIA, which consists of a procedure of passive adsorption of antibody molecules. Many approaches first employed in immunoassay now have been used in the fabrication of immunosensor devices.

Physical adsorption is the simplest way to immobilize antibodies on surface. However, the binding to surface is usually not stable, and the activity of the antibody is usually lost. For this reason, adsorption has to be controlled carefully. Concentrated antibody solutions should be avoided since additional layering will occur. Additional adsorption usually involves protein-protein adsorption rather than surface-protein adsorption. Such adsorption is inherently unstable, and the protein may gradually peel off during assay.

Due to SAMs' superb control over surface structure and properties, a combination of physical adsorption and SAMs have been used to immobilize proteins on surface. Liu, et al.[54] immobilized bovine serum albumin (BSA), lysozyme (LYZ) and rabbit Immunoglobulin G (IgG) onto methyl-, hydroxyl- and carboxylate- terminated SAMs by physical adsorption. It was found that at isoelectric point (IEP), protein readily adsorbs

on SAMs surface with 90% coverage. Different surface functionalities can result in the variation of morphology of adsorbed protein layers. The selectivity of protein immobilization can be controlled by choosing SAM terminal functionality and solution pH. The immobilized proteins are stable enough to sustain washing by water and buffer solution. Zhou and Abell[55] combined nanografting and electrostatic immobilization in construction of protein surface nanostructure. Three proteins, lysozyme, rabbit IgG, and bovine carbonic anhyrase were immobilized onto charged nanopatches at a variety of pH values.

1.4.2 Covalent immobilization

Covalent immobilization of antibodies on surfaces is based on the linkage between surface and antibody functional groups. Generally, there are three different approaches to attach proteins to surface other than physical adsorption. The first approach is to modify the SAMs substrate, then attach proteins to the substrate. The second approach is to link the protein of interest to sulfur-containing molecules. The modified protein is then self-assembled onto gold substrate through gold-thiol linkage. The third approach is to immobilize protein through a lock and key interaction, or ligand/receptor mechanism.

To understand the functional groups on antibodies, it is necessary to understand the structure of antibodies. Figure 1.4 shows a typical structure of an IgG molecule. Antibody molecules have the same basic structure. Each antibody consists of two identical light chains (~ 24 kDa) and two identical heavy chains (55 kDa or 70 kDa) covalently held together by disulfide bonds. The light chains are covalently attached to

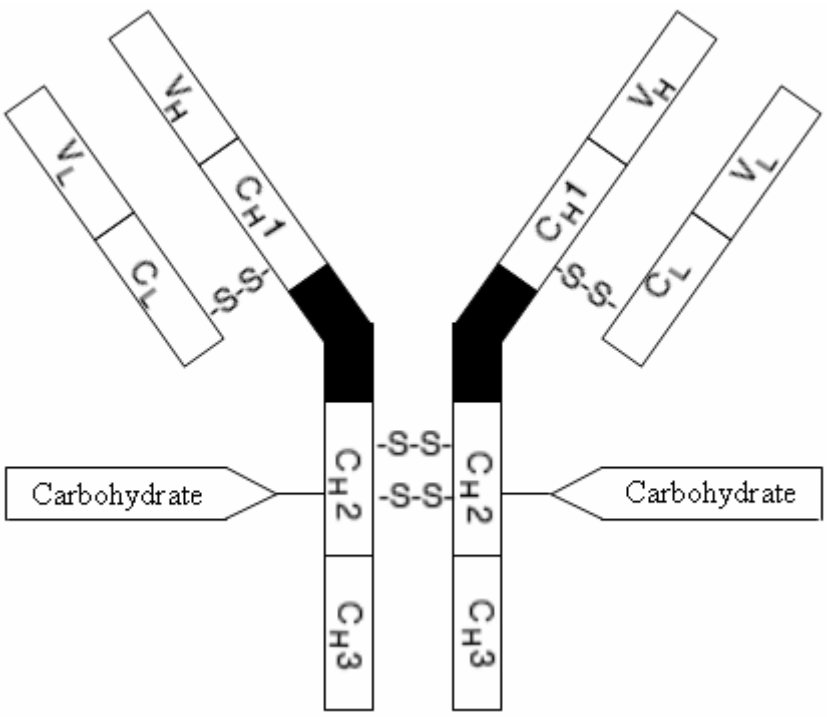

Figure 1.4 Structure of a typical IgG molecule

the heavy chains by disulfide bonds in the constant region of the light chain and heavy chain, while the heavy chains are covalently linked to each other through disulfide bonds in the hinge region.

From the antibody molecular structure, it can be seen that some of the antibody functionalities are available for immobilization. An antibody may be coupled through amine functional groups on lysine or N-terminal amines or carboxylic residues. Or, antibody fragments can be coupled through thiol groups after being cleaved enzymatically. Alternatively, mild oxidation of the carbohydrates at the Fc region can provide formyl groups for immobilization.

One of the major drawbacks of covalent immobilization is that it could result in a loss of activity. In order to preserve protein binding activity, several immobilization techniques have been developed so that antibodies can be attached in certain orientation. In the following text, these immobilization methods will be discussed in detail.

1.4.2.1 Random immobilization

There are 60-80 lysines distributed all over the immunoglobulin molecule. Antibody molecules can be covalently attached to surface functional groups through the amine groups. The abundance of amino groups on an antibody makes it possible to form a layer of dense proteins on the surface.[56, 57] However, due to the random nature of the antibody immobilization, although large surface protein density can be achieved, some activity might be lost after immobilization.

1.4.2.2 Site-directed immobilization

Antibodies produced in mammals are always glycosylated. The carbohydrate chains are attached to the C_H2 domain of the Fc portion of the antibody, situated far away

from the antigen binding site. Mild oxidation of the sugar residues using sodium periodate generates a formyl group. The formyl functional group can be coupled to an amine functional group on solid support. Hence, the antibody can be specifically immobilized through the modified carbohydrate residues. Antigen binding sites are less sterically hindered in this approach than when using random immobilization, giving the highest yield of antigen binding site activity close to the theoretical maximum 1:2, i.e. two antigen molecules binds to one immunoglobulin.

1.4.2.3 Use of specially-located thiol group on antibodies

The heavy chains of IgG molecules are linked together in the hinge region through disulfide bonds, which can be selectively reduced using 2-mercaptoethylamine (2-MEA), generating specifically located thiol groups. The thiol groups can be subsequently coupled to the activated surface. Antibodies can hence be immobilized with antigen binding sites facing away from the surface. An alternative approach is to digest the antibody with pepsin to produce a $F(ab)_2$ fragment, which is subsequently reduced using the above method to produce Fab' fragment with thiol groups available for coupling. The removal of the Fc fragment reduces non-specific binding. In addition, attachment through spontaneous chemisorption to gold substrates eliminates the need for chemical linkers and simplifies the immobilization process. Porter, et al.[58] constructed a miniaturized antigenic patterned array of immunosurface composed of spontaneously adsorbed rabbit Fab'-SH fragments. According to Thin-Layer spectroscopy, AFM, and confocal laser microscopy studies, it was found that an antigenic Fab'-SH monolayer on gold contains four times more intact epitopes per square centimeter than an antigenic monolayer of whole molecule antibodies.

1.4.2.4 Immobilization using adsorbed proteins

For antibody immobilization, the main concern lies on the retention of antigen binding activity. Antigen binding activity may be lost if the antibody binding site is blocked even if the antibody is not denatured. Some proteins can bind to the antibody in a certain direction so that the antigen binding site will not be obstructed. By orienting antibodies away from Fc portion, the binding activity is increased.

A wide range of immunoglobulin-binding molecules available for purification of antibodies in affinity chromatography can be adapted to immobilized proteins on surfaces. An obvious example is the antibody against the immunoglobulin, i.e., a secondary antibody. Some proteins, isolated from bacteria, have immunoglobulin-binding ability and they are more frequently used. The best known examples are Protein A and Protein G.[59]

Protein A is a 42 kDa surface protein from *Staphylococcus aureus*. The binding of Protein A to immunoglobulins usually occurs specifically through the Fc protion of the antibodies. However, the use of Protein A to immobilize protein works well only if there is no immunoglobulin in the antigen solution specific to protein A.

Protein G is a 30-35 kDa surface protein of *Streptococcus*. Protein G binds to a wide spectrum of antibodies, primarily through their Fc regions, although some evidence showed that Protein G interacts with Fab as well.

Protein A/G, a Fc binding fusion protein originating from gene fusion of the Fc binding domains of protein A and protein G, is a protein that combines the advantages, affinities, and specificities of both protein A and protein G.

Protein A or G can be immobilized on sensor surface through their amine groups and can function as capture proteins. However, if the capture proteins are immobilized randomly, not all of them can bind antibody. This may result in high antigen binding activity but low antibody density.

The most important property of using Protein A, G or A/G, is perhaps the ability to remove the active antibody layer and replace it with a different one under rather mild conditions.[60] The antibody-binding protein surface can act as a generic immunosensor platform. The specificity can be controlled by binding antibodies of interest. Compared to covalently immobilized antibodies that need to break the antibody-antigen complex to regenerate the surface, the antibody-binding protein immunosensor surface can be regenerated by desorbing antibody from the binding protein (by using buffer such as 20 mM citrate pH 3.5). This generates much more reproducible surfaces without causing biomolecule degradation.

1.4.2.5 Use of the immobilized Avidin, Streptavidin

Streptavidin is a ~60 kDa protein isolated from *Streptomyces avidinii*. Streptavidin is a tetrameric protein, with each subunit able to bind a single biotin molecule. Biotin, also known as Vitamin H, is a 244 Da vitamin found in tissue and blood, which binds with high affinity to streptavidin. In fact, the streptavidin-biotin interaction is the strongest known non-covalent biological interaction ($K_a = 10^{15}$ M^{-1}) between protein and ligand. The bond formation between streptavidin and biotin is rapid and essentially non-reversible; it is unaffected by most extremes of pH, organic solvents, and denaturing reagents. Extensive chemical modification has little effect on the activity of the protein. The streptavidin-biotin interaction has found extensive use as a research

tool. A variety of molecules, including lectins, proteins, and antibodies, can be biotinylated and reacted with streptavidin labeled probes or other detection reagents for use in biological assays. Peluso[61] investigated the effects of the orientation of the capture agents on the surface with two types of streptavidin-coated monolayer surfaces. It was found that the specific orientation of capture agents consistently increases the analyte-binding capacity of the surfaces, with up to 10-fold improvements over surfaces with randomly oriented capture agents.

The research on antibody immobilization onto surface has been studied for over forty years. It is impossible to cover all the immobilization techniques in this review. In today's literature, some other immobilization methods, such as use of tags with engineered antibody fragments and the use of randomly immobilized Fab fragment, are still in use to construct biosensors.

1.5 Modern microscopy: tools for biosensor research

Understanding the effects of different morphologies may lead to a process for enhancement of a given morphology, and therefore, to improved reactive selectivities and product yields. In biosensor development, immobilization of bioreceptors and molecular recognition events occur at the transducer surface. Visualization of transducer morphology can certainly help to better understand immobilization chemistry and molecular recognition events. Microscopy is an invaluable tool for acquisition of morphology. Surface microscopy serves two independent functions of enlargement (magnification) and improved resolution (the rendering of two objects as separate entities).

Depending on the selectivity and experimental conditions, the methods of microscopy may be varied. Knowledge of microscopy, hence, is important when studying a surface of interest. In the following text, a brief discussion of microscopy for biosensor research will be given.

1.5.1 Optical microscopy and electron microscopy

The elements of an optical microscope consist of light source, optics and magnification. Modern optical microscopy has been optimized to near perfection (maximum 1000×). However, the limits of resolution are set by fundamental laws in physics. The diffraction limit for maximal resolution is set by the wavelength of light 100 nm in ultra UV, 250 nm in immersed oil.

Electrons are particles that can be accelerated, focused, and detected. These particles have a shorter wavelength than visible light, giving higher resolution than that in optical microscopy.

The transmission electron microscope (TEM) is conceptually similar to the transmission optical microscope, in the arrangement of specimen, “light source”, and image plane, with the difference that electrons instead of light are used, electrostatic and magnetic lenses replace glass lenses, and detection is done with a fluorescent screen. Transmission electron microscope is capable of magnifying approximately 200,000 times with a resolution limit for biological specimens of about 1 nm.

Another important type of microscope is the scanning electron microscope (SEM). In SEM, the electron beam is focused onto a small spot and scans a parallel linear scans over the surface of the specimen. The electrons that are going back out from the surface

are detected simultaneously with an electron detector. The resolution of the scanning electron microscope is about 6 nm.

Electron microscopy has wide applications in imaging conducting materials. For non-conducting materials, a layer of conductive coating needs to be coated to the sample surface before imaging. Due to the inherent limitation of electron microscopy, more than two decades ago a new procedure for molecular microscopy was invented: scanning probe microscopy.

1.5.2 Scanning probe microscopy (SPM)

Scanning probe microscopy is unique amongst all imaging techniques. It provides three-dimensional real-space images and allows localized measurements of structures and properties with high resolutions. When samples are ultraflat, atomic resolution can be achieved. Depending on the particular SPM, the image can represent surface topography, electronic structure, electric or magnetic fields. For macromolecules and biological tissues, SPM achieves high resolution without destroying samples. In contrast to electron microscopy, SPM images can be acquired at ambient conditions rather than high vacuum conditions.

Scanning probe microscopy can be further categorized to Scanning Tunneling Microscopy (STM) or Scanning Force Microscopy (SFM).

The scanning tunneling microscope was invented by Binnig and Rohrer in 1982. Later, the atomic force microscope was developed based on the principles of STM but with resolving surface structure for nonconducting and conducting materials.

The principle of scanning probe microscopy is that a sharp tip moves over the surface with a piezoelectric sensor of molecular scale sensitivity in the longitudinal and height directions maintaining a feedback loop, keeping either the tunneling current or the force constant. Since the focus of this review is on nonconductive material (biological samples), emphasis will be given to Atomic Force Microscope (AFM).

1.5.2.1 Atomic Force Microscopy (AFM)

AFM works by scanning a sharp tip on the end of a flexible cantilever across a sample surface while maintaining a small constant force between the tip and surface. The scanning motion is achieved by a piezoelectric tube scanner which scans the tip in a raster pattern with respect to the sample. The vertical tip-sample interaction is monitored by reflecting a laser off the back of the end of the cantilever into a photodiode detector. By detecting the difference in the photo detector output voltages, changes in the cantilever deflection or oscillation amplitude are determined. Generally, there are three most commonly used modes of operation: contact mode AFM, tapping mode AFM, and non-contact AFM.

Contact mode AFM works by scanning the cantilever tip across the sample surface while recording the change in cantilever deflection with the photodiode detector. A feedback loop maintains a constant cantilever deflection by vertically moving the scanner to maintain a constant photo detector difference signal. The distance the scanner moved vertically is used to generate the topographic image of the sample surface. This feedback loop maintains a constant force during image acquisition, which typically ranges 0.1 - 100 nN.

Tapping mode AFM and non-contact AFM work by oscillating the cantilever at its resonance frequency. In tapping mode AFM, the tip is slightly tapping the sample surface during image acquisition, while in non-contact AFM, the tip does not contact the sample surface at all. In both modes, the laser deflection method is used to detect the amplitude of cantilever oscillation. The feedback loop maintains a constant oscillation amplitude by moving the scanner vertically at every x y data point. Recording this movement forms the topographic image.

Selection of operating mode depends on sample properties and experimental objectives. In tapping mode and non-contact mode AFM, lateral force and shear force are eliminated so deformation and destruction of biological samples can be prevented. Therefore, these modes are suitable for soft surface imaging. In the past decade, AFM has had great success in imaging biological samples, such as DNA,[62-66] lipids, proteins and living cells.

DNA is a large molecule. Imaging of covalent immobilization of modified DNA fragments on gold revealed the substructure of the linear DNA molecules by AFM.[63] A high-resolution image of DNA was obtained when DNA was tightly adsorbed onto a cationic layer and imaged by contact mode AFM.[62] The helical repeat of the major groove of the double helix was observed at many places in the image.

Lipids are relatively small molecules. Immobilized on SAMs, a well-defined hexagonal structure was seen for a C-18 chain length.[75] SAMs of artificial thiolipid on gold appeared as star-like domain structures.[76]

Proteins are the most studied molecules in biomedical sciences. Since they are the final product of gene expression, they are usually the interventional target in

pharmaceutical research. The most useful tool to elucidate protein structures are X-ray diffraction of protein crystals and 2D-NMR. As a complementary tool, AFM has been used to investigate protein assemblies at physiological conditions. Bacteriorhodopsin on mica was shown to form a regular layer where individual molecules could clearly be identified.[76] Single large molecules of an intracellular protein transport system were covalently bonded on mica and the Y-shaped structure was found as predicted by electron microscopy.[77]

AFM can not only provide high-resolution images, but can also detect the forces between molecules at the single molecular level. AFM is able to generate a force-distance (F/D) curve. Binding or unbinding force values can be determined from the F/D curves, which can be used for analytical purposes. Typical examples are the force study by AFM between avidin-biotin, antigen-antibody, DNA-DNA, etc. The study of forces facilitates the understanding of biomolecular interaction processes on the single molecular level.

The high binding constant between avidin or streptavidin and biotin provide a good model system for AFM force study. A binding force of 160 pN was determined for a single avidin-biotin interaction.[78] The good correlation of binding force values to energy change indicated that the dissociation process is adiabatic, and entropic changes may occur after the dissociation process is finished.

Antibody-antigen binding is an important process of immunological responses. Early studies by AFM concluded a single rupture force of 60±10 pN.[79] When a monovalent single chain fragment in the variant region was immobilized on gold through a C-terminal cysteine at a low surface density, a tip with covalently attached antigen molecules showed a Gaussian distribution of unbinding force with a mean 50±4 pN.[80]

Other forces, such as cell adhesion, intramolecular forces in protein and polysaccarides have been studied by AFM F/D methods. A more complete discussion of AFM force study on biological samples can be found in other reviews.[81-83]

Various microscopic techniques have different resolutions and generate different views of the cell. The limit of resolution of a light microscope is about 0.2 μm; of a transmission electron microscope, about 1 nm; and of a scanning electron microscope, about 10 nm. Scanning probe microscopy can resolve to the atomic scale. It is essential to know which imaging technique to use for a specific living organism. Table 1.2 showed the appropriate technique for imaging living organisms.

1.6 Conclusion

One of the greatest challenges in biosensor development is the proper immobilization of the biological recognition element while preserving its activity. A number of methods for immobilizing and orienting antibodies were described. Self-assembled monolayers having superb control over surface structure and property, provide an ideal platform for biosensor construction. Modern microscopy, especially atomic force microscopy, plays an essential role in biosensor development.

Table 1.2 Summary of microscopy for imaging biological samples

Biological Sample	Approximate Size	AFM	Electron Microscopy	Light Microscopy
DNA	2 nm	×		
Antibody	5 nm	×		
Cell membrane	7-10 nm	×		
Ribosome	25 nm	×	×	
Large virus	100 nm	×	×	
Bacteria	1-5 μm		×	×
Chloroplast	2-10 μm		×	×
Typical animal cells	10 – 30 μm		×	×
Typical plant cells	10- 100 μm		×	×
Human egg	100 μm		×	×

1.7 References

(1) Schultz, R. F. T. a. J. S., Ed. *Handbook of chemical and biological sensors*; Institute of Physics Publishing: Philadelphia, 1996.

(2) Turner A.P.F., K. I., Wilson G.S. *Biosensors: Fundamentals and Applications*; Oxford University Press: Oxford, 1989.

(3) Clark, L. C., Jr.; Lyons, C. *Ann. N. Y. Acad. Sci.* **1962**, *102*, 29-45.

(4) Updike, S. J.; Hicks, G. P. *Nature* **1967**, *214*, 986-988.

(5) Eggins, B. R. *Chemical Sensors and Biosensors*; John Wiley & Sons, Inc.: New York, NY, 2002.

(6) Editor: Narayanaswamy, R.; *Optical Chemical Sensors and Biosensors, (Proceedings of the 6th European Conference held in Manchester, UK 7-10 April 2002.)*; Lyon - Villeurbanne, France, 2003.

(7) Cattrall, R. W. *Chemical Sensors*; Oxford University Press Inc.: New York, NY, 1997.

(8) Spichiger-Keller, U. E. *Chemical Sensors and Biosensors for Medical and Biological Applications*; Wiley / VCH: Weinheim, 1997.

(9) Wolfbeis, O. *Mikrochim. Acta.* **1995**, 1-4.

(10) Editor: Roberts, G.; *Langmuir-Blodgett Films*; Plenum Press: New York., 1990.

(11) Love, J. C.; Gates, B. D.; Wolfe, D. B.; Paul, K. E.; Whitesides, G. M. *Nano Lett.* **2002**, *2*, 891-894.

(12) Fukushima, H.; Seki, S.; Nishikawa, T.; Takiguchi, H.; Tamada, K.; Abe, K.; Colorado, R., Jr.; Graupe, M.; Shmakova, O. E.; Lee, T. R. *J. Phys. Chem. B* **2000**, *104*, 7417-7423.

(13) Peters, R. D.; Yang, X. M.; Kim, T. K.; Sohn, B. H.; Nealey, P. F. *Langmuir* **2000**, *16*, 4625-4631.

(14) Fujihira, M.; Tani, Y.; Furugori, M.; Okabe, Y.; Akiba, U.; Yagi, K.; Okamoto, S. *Stud. Surf. Sci. Catal.* **2001**, *132*, 469-476.

(15) Chapman, R. G.; Ostuni, E.; Liang, M. N.; Meluleni, G.; Kim, E.; Yan, L.; Pier, G.; Warren, H. S.; Whitesides, G. M. *Langmuir* **2001**, *17*, 1225-1233.

(16) Kim, S.; Choi, G. Y.; Nezaj, J.; Ulman, A.; Fleischer, C. *Macromolecular Symposia* **1998**, *126*, 1-6.

(17) Kong, D.; Wan, L.; Chen, S.; Yang, W. *Fushi Yu Fanghu* **2003**, *24*, 415-420.

(18) Kong, Y.; Zhang, S.-Y.; Li, H.-J. *Huaxue Xuebao* **2004**, *62*, 1612-1616.

(19) Whelan, C. M.; Kinsella, M.; Ho, H. M.; Maex, K. *J. Electrochem. Soc.* **2004**, *151*, B33-B38.

(20) Vaidya, R. U.; Brozik, S. M.; Deshpande, A.; Hersman, L. E.; Butt, D. P. *Metall. Trans. A* **1999**, *30A*, 2129-2134.

(21) Li, X.-M.; Peter, M.; Huskens, J.; Reinhoudt, D. N. *Nano Lett.* **2003**, *3*, 1449-1453.

(22) Stolarczyk, K.; Bilewicz, R. *Electroanalysis* **2004**, *16*, 1609-1615.

(23) Santhanam, V.; Andres, R. P. *Nano Lett.* **2004**, *4*, 41-44.

(24) Lee, W.; Kim, E. R.; Lee, H. *Langmuir* **2002**, *18*, 8375-8380.

(25) Park, J. W.; Maeng, I. S.; Chung, Y. J. *Hwahak Sekye* **2003**, *43*, 35-38.

(26) Austin, M. D.; Chou, S. Y. *Nano Lett.* **2003**, *3*, 1687-1690.

(27) Kraemer, S.; Fuierer, R. R.; Gorman, C. B. *Chem. Rev.* **2003**, *103*, 4367-4418.

(28) Chaki, N. K.; Vijayamohanan, K. *Biosens. Bioelectron.* **2002**, *17*, 1-12.

(29) Wink, T.; van Zuilen, S. J.; Bult, A.; van Bennkom, W. P. *Analyst* **1997**, *122*, 43R-50R.

(30) Vijayamohanan, K.; Aslam, M. *Appl. Biochem. Biotechnol.* **2001**, *96*, 25-39.

(31) Bain, C. D.; Troughton, E. B.; Tao, Y. T.; Evall, J.; Whitesides, G. M.; Nuzzo, R. G. *J. Am. Chem. Soc.* **1989**, *111*, 321-335.

(32) Lu, G. H.; Liu, C. Y.; Zhao, H. Y.; Liu, W.; Jiang, L. P.; Jiang, L. Y. *Chin. Chem. Lett.* **2004**, *15*, 827-830.

(33) Nishiyama, K.; Kubo, A.; Ueda, A.; Taniguchi, I. *Chem. Lett.* **2002**, 80-81.

(34) Zhang, J.; Kirkham, J.; Robinson, C.; Wallwork, M. L.; Smith, D. A.; Marsh, A.; Wong, M. *Anal. Chem.* **2000**, *72*, 1973-1978.

(35) Luo, L.-Q.; Zhao, J.-W.; Yang, X.-R.; Wang, E.-K.; Dong, S.-J. *Gaodeng Xuexiao Huaxue Xuebao* **2000**, *21*, 380-382.

(36) Luo, L.-Q.; Cheng, Z.-L.; Yang, X.-R.; Wang, E.-K. *Chinese Journal of Chemistry* **2000**, *18*, 863-867.

(37) Zhao, J. W.; Luo, L. Q.; Yang, X. R.; Wang, E. K.; Dong, S. J. *Electroanalysis* **1999**, *11*, 1108-1111.

(38) Smalley, J. F.; Chalfant, K.; Feldberg, S. W.; Nahir, T. M.; Bowden, E. F. *Journal of Physical Chemistry B* **1999**, *103*, 1676-1685.

(39) Shimazu, K.; Teranishi, T.; Sugihara, K.; Uosaki, K. *Chem. Lett.* **1998**, 669-670.

(40) Creager, S. E.; Clarke, J. *Langmuir* **1994**, *10*, 3675-3683.

(41) Wang, J.; Frostman, L. M.; Ward, M. D. *J. Phys. Chem.* **1992**, *96*, 5224-5228.

(42) Hu, K.; Bard, A. J. *Langmuir* **1997**, *13*, 5114-5119.

(43) Tsukruk, V. V.; Bliznyuk, V. N.; Wu, J. *ACS Symp. Ser.* **1998**, *694*, 321-341.

(44) Noy, A.; Vezenov, D. V.; Rozsnyai, L. F.; Lieber, C. M. *J. Am. Chem. Soc.* **1997**, *119*, 2006-2015.

(45) Godinez, L. A.; Castro, R.; Kaifer, A. E. *Langmuir* **1996**, *12*, 5087-5092.

(46) Mayya, K. S.; Patil, V.; Sastry, M. *Langmuir* **1997**, *13*, 3944-3947.

(47) Chechik, V.; Crooks, R. M.; Stirling, C. J. M. *Advanced Materials* **2000**, *12*, 1161-1171.

(48) Mikolajczyk, M.; Kielbasinski, P. *Tetrahedron* **1981**, *37*, 233-284.

(49) Frey, B. L.; Corn, R. M. *Anal. Chem.* **1996**, *68*, 3187-3193.

(50) Ostuni, E.; Grzybowski, B. A.; Mrksich, M.; Roberts, C. S.; Whitesides, G. M. *Langmuir* **2003**, *19*, 1861-1872.

(51) Nelson, K. E.; Gamble, L.; Jung, L. S.; Boeckl, M. S.; Naeemi, E.; Golledge, S. L.; Sasaki, T.; Castner, D. G.; Campbell, C. T.; Stayton, P. S. *Langmuir* **2001**, *17*, 2807-2816.

(52) Frederix, F.; Bonroy, K.; Laureyn, W.; Reekmans, G.; Campitelli, A.; Dehaen, W.; Maes, G. *Langmuir* **2003**, *19*, 4351-4357.

(53) Datwani, S. S.; Vijayendran, R. A.; Johnson, E.; Biondi, S. A. *Langmuir* **2004**, *20*, 4970-4976.

(54) Wadu-Mesthrige, K.; Amro, N. A.; Liu, G.-Y. *Scanning* **2000**, *22*, 380-388.

(55) Zhou, D.; Wang, X.; Birch, L.; Rayment, T.; Abell, C. *Langmuir* **2003**, *19*, 10557-10562.

(56) Li, L.; Chen, S.; Oh, S.; Jiang, S. *Anal. Chem.* **2002**, *74*, 6017-6022.

(57) Patel, N.; Davies, M. C.; Hartshorne, M.; Heaton, R. J.; Roberts, C. J.; Tendler, S. J. B.; Williams, P. M. *Langmuir* **1997**, *13*, 6485-6490.

(58) O'Brien, J. C.; Jones, V. W.; Porter, M. D.; Mosher, C. L.; Henderson, E. *Anal. Chem.* **2000**, *72*, 703-710.

(59) Breitling, F.; Subel, S. *Recombinant Antibodies*; John Wiley and Sons: New York, 1999.

(60) Pei, R.-J.; Hu, J.-M.; Hu, Y.; Zeng, Y. e. *Journal of Chemical Technology & Biotechnology* **1998**, *73*, 59-63.

(61) Peluso, P.; Wilson, D. S.; Do, D.; Tran, H.; Venkatasubbaiah, M.; Quincy, D.; Heidecker, B.; Poindexter, K.; Tolani, N.; Phelan, M.; Witte, K.; Jung, L. S.; Wagner, P.; Nock, S. *Anal. Biochem.* **2003**, *312*, 113-124.

(62) Mou, J.; Czajkowsky, D. M.; Zhang, Y.; Shao, Z. *FEBS Lett.* **1995**, *371*, 279-282.

(63) Hegner, M.; Wagner, P.; Semenza, G. *FEBS Lett.* **1993**, *336*, 452-456.

(64) Chen, X.; Zhang, Y.; Hu, J.; Wu, S.; Huang, Y.; Ai, X.; Qiu, X.; Li, M. *Hejishu* **2001**, *24*, 630-635.

(65) Chen, L.; Haushalter, K. A.; Lieber, C. M.; Verdine, G. L. *Chemistry & Biology* **2002**, *9*, 345-350.

(66) Kawaura, C.; Furuno, T.; Nakanishi, M. *Bioimages* **1997**, *5*, 121-125.

(67) Kim, J. M.; Jung, H. S.; Park, J. W.; Lee, H. Y.; Kawai, T. *Anal. Chim. Acta* **2004**, *525*, 151-157.

(68) Morii, T.; Mizuno, R.; Haruta, H.; Okada, T. *Thin Solid Films* **2004**, *464-465*, 456-458.

(69) Pastushenko, V. P.; Kaderabek, R.; Sip, M.; Borken, C.; Kienberger, F.; Hinterdorfer, P. *Single Molecules* **2002**, *3*, 111-117.

(70) Qu, M.-H.; Li, H.; Tian, R.; Nie, C.-L.; Liu, Y.; Han, B.-S.; He, R.-Q. *NeuroReport* **2004**, *15*, 2723-2727.

(71) Xu, X.-M.; Ikai, A. *Anal. Chim. Acta* **1998**, *361*, 1-7.

(72) Yu, L.-h.; Li, Z.; Wu, A.-g.; Wang, H.-d.; Suo, Q.-l.; Bi, X.-h.; Huang, B.-q. *Gaodeng Xuexiao Huaxue Xuebao* **2002**, *23*, 46-48.

(73) Yuan, M.; Hou, Z.; Feng, W.; Zhang, Z.; Wei, H. *High Tech. Lett.* **2001**, *7*, 6-7.

(74) Zheng, J.; Li, Z.; Wu, A.; Zhou, H. *Biophys. Chem.* **2003**, *104*, 37-43.

(75) Alves, C. A.; Smith, E. L.; Porter, M. D. *J. Am. Chem. Soc.* **1992**, *114*, 1222-1227.

(76) Stamou, D.; Gourdon, D.; Liley, M.; Burnham, N. A.; Kulik, A.; Vogel, H.; Duschl, C. *Langmuir* **1997**, *13*, 2425-2428.

(77) Wagner, P.; Kernen, P.; Hegner, M.; Ungewickell, E.; Semenza, G. *FEBS Lett.* **1994**, *356*, 267-271.

(78) Moy, V. T.; Florin, E.-L.; Gaub, H. E. *Science* **1994**, *266*, 257-259.

(79) Dammer, U.; Hegner, M.; Anselmetti, D.; Wagner, P.; Dreier, M.; Huber, W.; Guentherodt, H. J. *Biophys. J.* **1996**, *70*, 2437-2441.

(80) Ros, R.; Schwesinger, F.; Anselmetti, D.; Kubon, M.; Schafer, R.; Pluckthun, A.; Tiefenauer, L. *Proc. Natl. Acad. Sci. U. S. A.* **1998**, *95*, 7402-7405.

(81) Allen, S.; Rigby-Singleton, S. M.; Harris, H.; Davies, M. C.; O'Shea, P. *Biochem. Soc. Trans.* **2003**, *31*, 1052-1057.

(82) Hugel, T.; Seitz, M. *Macromolecular Rapid Communications* **2001**, *22*, 989-1016.

(83) Willemsen, O. H.; Snel, M. M. E.; Cambi, A.; Greve, J.; De Grooth, B. G.; Figdor, C. G. *Biophys. J.* **2000**, *79*, 3267-3281.

CHAPTER 2 COVALENT IMMOBILIZATION OF ANTIBODIES ON SELF-ASSEMBLED MONOLAYER SURFACES AND CHARACTERIZATION WITH NON-CONTACT ATOMIC FORCE MICROSCOPY

2.1 Introduction

The development of biosensor,[1-10] protein microarray[11-23] and other diagnostic immunoassay technologies demands the immobilization of proteins on surfaces while retaining their activity and stability. The successful implementation of these technologies is totally dependent on optimized methods of protein immobilization.

Protein immobilization methodologies on solid supports, especially on gold substrates, have been the interest of considerable research efforts. Most of today's protein immobilization methodologies were developed from that of affinity chromatography.[24-29] A successful protein immobilization approach would require the immobilized protein to be controlled in an optimized orientation so that the active binding site would be accessed without much hindrance. At the same time, the antibody surface density needs to be maximized, preferably well-controlled. The most commonly used methods are physical adsorption, entrapment and covalent attachment.[30-34] Physical adsorption of protein to surface is the most direct and simple approach. However, it often results in denaturation and partial loss of activity. Physical entrapment and cross-linking cannot control protein

orientation on surface. Proteins can be directly coupled to amine-reactive surfaces with proper terminal functional groups. Compared to physical adsorption, less protein might be denatured when immobilized onto surface. However, random immobilization causes the attached protein to lose binding activity. Due to the random nature of the immobilization methods, the antigen-binding sites may be modified or sterically hindered either by the surface or adjacent antibodies. In order to increase the accessibility of binding sites, it is of great importance to create oriented proteins so that the immobilized antibody binding sites are oriented away from the surface.

Based on the functionalities on the antibody molecule, the antibody could be immobilized in certain orientations. Antibody fragments Fab or $F(ab')_2$ can be coupled after being cleaved enzymatically. The Fab or $F(ab')_2$ binding site is positioned away from the surface by coupling the sulfhydryl moiety located on the fragment's C-terminus to the substrate. Antibodies can also be oriented and immobilized through antibody-binding Protein A, Protein G or by engineering protein histidine. Additionally, they can also be immobilized through the carbohydrate moiety on the antibody Fc region to the substrate.

The ease of preparation, the strength of the bond formed between sulfur and the metal, and a wide range of terminal functional groups in the adsorbing molecule[35-38] make self-assembled monolayers (SAMs) a promising platform for antibody immobilization. For mixed SAMs, when both molecules are present in the deposition solution, the mole fraction of each molecule in the SAMs can be controlled through the mole ratio of the two molecules in the solution. When the monolayers are tailored with functional terminal groups, it is possible to control chemical and structural properties by

adjusting the tail groups.[39, 40] The combination of SAM platforms and protein immobilization make it possible to control the surface density of proteins.[39-45] A number of SAMs are now available that resist adsorption of protein, such as SAMs terminating in hydroxyl or ethylene glycol groups.[46-49] The incorporation of such thiol and a functional end group in a mixed SAMs enables the attachment of receptor molecules and induces specific interaction of the immobilized protein instead of nonspecific adsorption of undesired biomolecules on the surface. According to STM studies,[50] when formed at room temperature, multi-component SAMs are phase-segregated and contain defects and small domains. At elevated solution temperatures, mixed SAMs are uniform and contain larger domains. It was also found that the time required to form the compact thin layer is greatly reduced at higher temperature.

Contact-mode AFM has been widely used in research. Contact mode is ideal for imaging hard surface since the cantilever tip is in contact with surface. Since the tip is rastered across the surface, when imaging soft samples, such as protein samples, the samples can easily be damaged. In contact-mode AFM, protein molecules are compressed under imaging conditions. The compressed heights were defined as the height of the initial and the final contact points of the tip on the protein. The compression is due to the mechanical force that is applied to the sample when imaging in contact mode. Even when samples were not seriously damaged, the cantilever tip often lasts only for a couple of scans and needs to be changed frequently. In order to avoid the laborious procedure of changing cantilevers tip and saving biological samples on surface from damaged, non-contact mode AFM (NC AFM) was adopted. Since the tip is not in direct contact with the sample, compression is almost undetectable.

In this chapter, the immobilization of antibodies through the Fc moiety of antibody onto an amine-terminated self-assembled monolayer on gold is reported. The carbohydrates on antibodies were oxidized by sodium periodate and –CHO groups were generated. The oxidized antibodies were subsequently covalently linked to self-assembled monolayers through Fc moiety. NC AFM was used to examine the gold surface.

2.2 Experimental

Chemicals. N-(3-Dimethylaminopropyl)-N'-ethylcarbodiimide hydrochloride (EDC), N-hydroxysuccinimide (NHS), 16-mercaptohexadecanoic acid, 11-mercapto-1-undecanol were obtained from Aldrich Chemical Company. Sodium periodate was obtained from Fisher Scientific. Antibody γ-chain specific (Immunoglobulin G or IgG) was obtained from Sigma Corporation.

Preparation of Au(111) substrate. Gold single crystal surfaces were prepared as described[51] previously. Au wire (Gold wire 99.999%, 0.762 mm/0.030 inch in diameter, Alfa) was cleaned by deionized water, absolute ethanol, piranha solution, deionized water and absolute ethanol sequentially. Then the gold wire was dried in a stream of dry Argon. The Au wire was melted in a H_2/O_2 flame and cooled in air in an up and down motion repeatedly until a gold ball with multiple facets formed at the end of the gold wire. The gold ball was annealed in a small hydrogen flame for 15 minutes prior to be used as substrate for self-assembled monolayers.

Formation of self-assembled monolayers. Self-assembled monolayers were formed by immersing gold in a mixture of 1mM alkanethiols in ethanol (0.01 mM 16-mercaptohexadecanoic acid and 0.99 mM 11-mercapto-1-undecanol) for 3 hrs at 60°C.[43] Upon removing the gold from solution, the samples were washed sequentially with absolute ethanol, 10% acetic acid and absolute ethanol and dried in a stream of Argon.

Activation of carboxylic acid functional groups. After self-assembled monolayer formation, the gold samples were immersed in 2 mg/mL EDC and 2 mg/mL NHS for 30 minutes. The samples were then taken out the solution, washed with deionized water, ethanol and then deionized water.

Antibody oxidation. The antibodies were oxidized according the procedure described in the literature.[52] 500 μL of 10 μg/mL antibody solution was added to 500 μL of 20 mM fresh sodium periodate solution at 0°C. After 20 minutes, the mixed solution was quenched with 6.5 μL glycerol. The solution was filtered by Microcon-50 microfilter at 3000 × g, and reconstituted to 5 μg/mL with 10 mM phosphate buffer saline (PBS) (pH 7.3).

Antibody immobilization. Antibodies were attached to the surface either through amine groups on antibodies or through Fc portion after oxidation. Random immobilization: Activated substrate was immersed into 5 μg/mL antibody solution in 10 mM PBS buffer (pH 7.3) overnight. Antibody immobilization through Fc portion: Activated substrate was immersed in 0.3 mg/mL adipic dihydrazide and 5 μg/mL oxidized antibody solution (pH 6.0) overnight. After immobilization, the samples were thoroughly washed with DI water and dried with Argon.

AFM imaging. All AFM images were acquired using an Atomic Force Microscope Autoprobe CP from Park Scientific, and an Acquisition Module from Thermomicroscope. The imaging probes were ULNC-AUMT-AB mounted silicon cantilevers with spring constant 2.1 N/m purchased from Digital Instruments. All images were acquired with a 100 μm Scanner Master at a scan rate of 0.6 Hz in non-contact mode in air at room temperature. The resonant frequency was set at 59 kHz. A video camera integrated with a microscopic objective piece was used to monitor laser beam location on the silicon cantilever.

Data Analysis. The particle diameter and height were measured with PSI ProScan 1.5 data analysis software. Line analysis allowed the horizontal section of an imaged particle to be viewed at a particular z height and defined the boundaries of the image of the particle based on z parameter.

2.3 Results and Discussion

Activation of SAMs. The first step of the reaction involves an activation step by EDC. EDC is a water-soluble carbodiimmide that has been widely used in peptide synthesis. In this work, a combination of EDC/NHS was used. EDC/NHS chemistry is chosen over EDC for two reasons. First, the intermediate -CO-NHS through EDC/NHS activation has a much longer half-life than that of EDC intermediate. Hence, it was more stable and less easily hydrolyzed. Second, EDC/NHS was chosen for compatibility reasons. It was found from experiments that acetate, phosphate and citrate buffers are not compatible with EDC. The combination of EDC and these buffers resulted in no protein

attachment. However, after forming intermediate -CO-NHS, acetate, phosphate and citrate buffer could be used to dispense antibody solution.

Protein immobilization. Mixed SAMs of carboxylic acid-terminated long-chain thiol (HS-C_{15}COOH) and hydroxyl-terminated short-chain thiol (HS-C_{11}OH) were used as a platform to covalently immobilize capture antibody to gold substrate in order to achieve more uniformly immobilized immunoreagent. 11-mercapto-1-undecanol was incorporated in SAMs to reduce non-specific adsorption. Hydroxyl-terminated alkanethiol resists protein adsorption as well as the family of poly(ethylene)glycol-terminated SAMs.[46, 49]

The reaction scheme of antibody immobilization on mixed SAMs is illustrated in Figure 2.1. Uniform mixed SAMs were formed on Au(111) substrate upon immersing in 16-mercaptohexadecanoic acid:11-mercapto-1-undecanol =1:99 ethanol solution for 3 h at 60°C. After being activated by EDC and NHS, the SAMs surface was ready to react with antibodies. For the random immobilization, the NHS intermediate was then reacted with lysine groups on the protein, forming amide bonds between the surface and proteins. For oriented immobilization, a bi-functional linker, adipic dihydrazide, was used to link the surface with the formyl group on the oxidized antibodies. The surface density of antibodies can be controlled through varying carboxylic acid composition in mixed SAMs.

The Au (111) surfaces were investigated by AFM at different stages of the immobilization process. AFM images of bare Au (111) surface (Figure 2.2) showed smooth terrace-step structure, the height of each step is in accordance with the monoatomic step height of 2.38 nm and the flat regions correspond to atomic flat

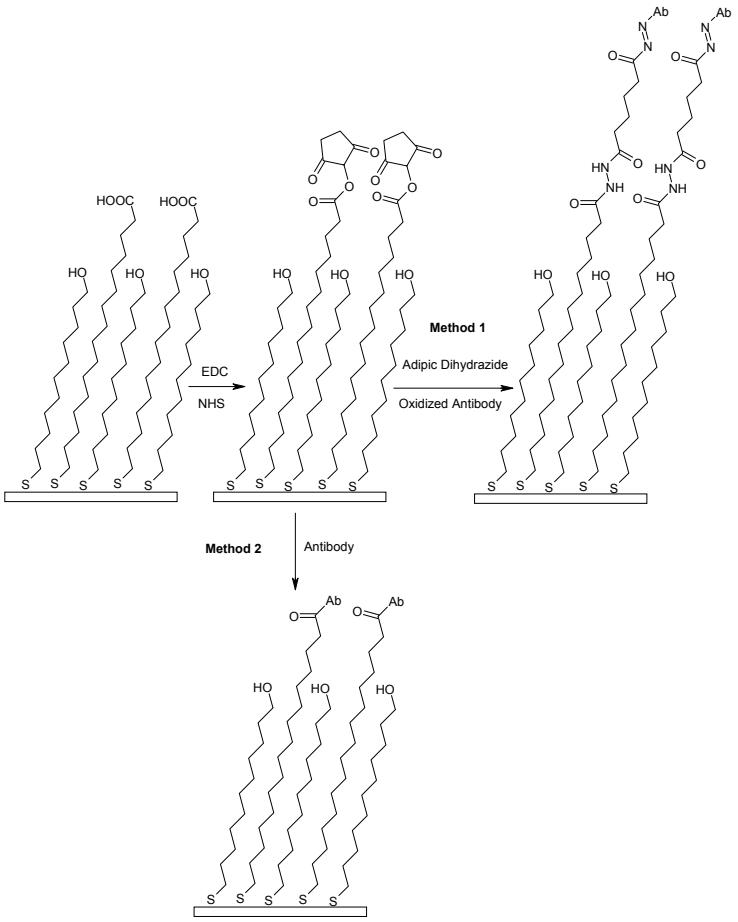

Figure 2.1 Reaction scheme of antibody immobilization on SAMs

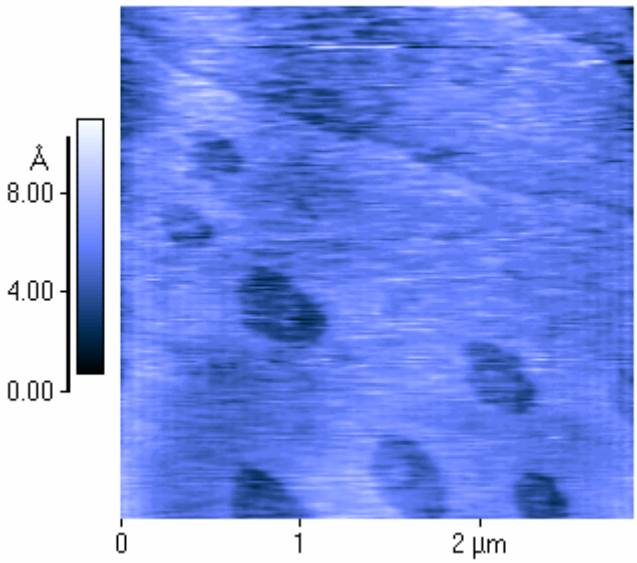

Figure 2.2 Contact-mode AFM topographical image of bare Au(111) surface

Au(111). Defects of monoatomic height were also found on Au(111) surface. AFM topographical image of mixed SAMs on Au(111) (Figure 2.3) revealed a flat, featureless surface with surface average roughness of 0.1 nm.

Non-specific adsorption was checked over 11-mercapto-1-undecanol SAMs. No obvious non-specific adsorption was found.

Figure 2.4 shows the AFM topographical image of Au (111) after the immobilization of antibody on SAMs (method 2). A change in topography is clearly observed in Figure 2.4. The height of the layer is approximately 4.0 nm, which is within the experimental error of an IgG molecule. Therefore, our data is consistent with a monolayer of the antibody being formed during the immobilization process. Formation of antibody monolayer was complete in 90 minutes. For convenience, the deposition time was extended to overnight.[53] Once the monolayer was formed, no further deposition of antibodies was observed to occur. Compared with SAMs of thioctic acid and butanethiol formed at room temperature with the same carboxylate composition ratio,[53] this SAM yielded much more dense antibodies on surface with an antibody density of 425 IgG molecules/μm^2. Uniform SAMs and less phase segregation lead to more available carboxylic acid groups on the surface, which yielded more attached protein on surface, despite the low carboxylic acid end functional group concentration on SAMs.

Figure 2.5 shows the NC AFM image when site-directed immobilization method (method 1) was used to attach antibody to gold. Bright, round spots of ~71 nm in diameter and ~3.1 nm in height can be clearly identified in the image. The immobilized IgG was imaged in air under ambient condition. Individual IgGs appear to be distinguishable in this image. After 5-10 scans, IgG molecules were not displaced from

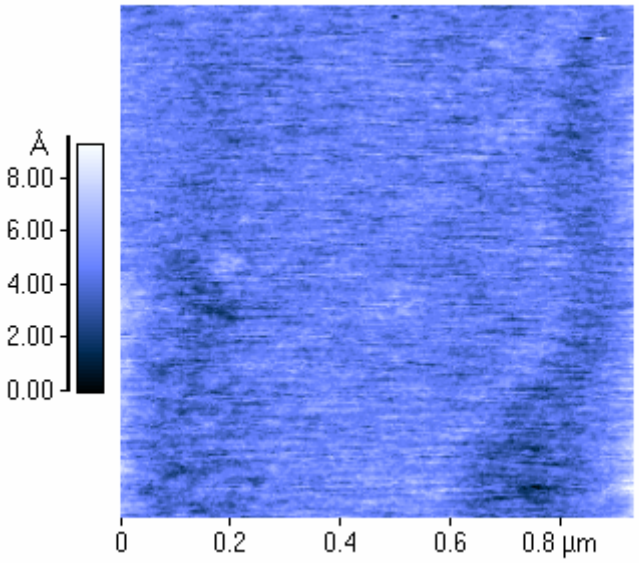

Figure 2.3 Contact-mode AFM topographical image of mixed SAMs

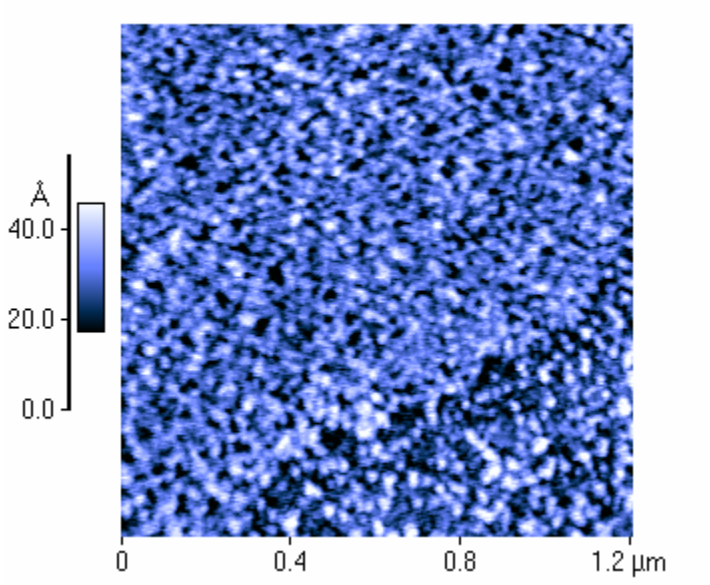

Figure 2.4 NC AFM topographical image of randomly immobilized antibodies on SAMs

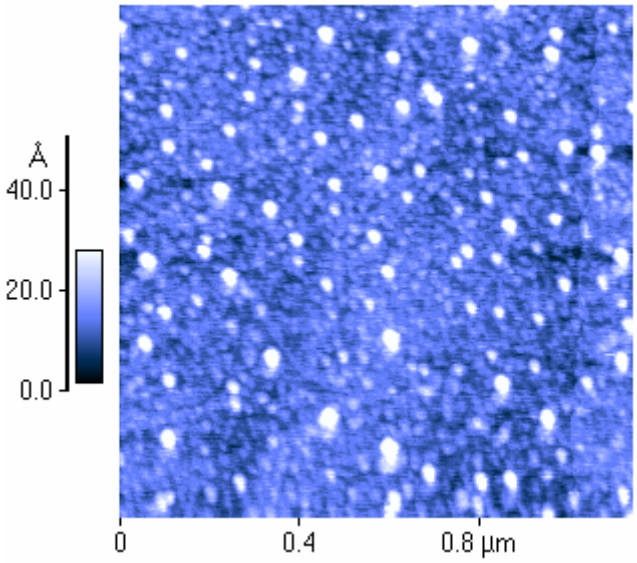

Figure 2.5 NC AFM topographical image of antibody immobilized through carbohydrate region on SAMs

the substrate, suggesting that the monolayers are stable. The apparent diameter of particles ranged in 71±8 nm, which represents approximately a 10-fold overestimation as compared with measurement by x-ray diffraction.[54-56] The height of particles ranges 3.1±0.6 nm, which is in agreement with that of IgGs. The IgG molecules in Figure 2.5 appear larger than in Figure 2.4 due to the different scan sizes.

Although vertical resolution is generally excellent, AFM can produce erroneous lateral feature dimensions due to the convolution of the geometry of the sample and the probe.[57] The NC-AFM in this study was operated in amplitude modulation AFM[58] mode. In this mode, the cantilever is oscillated near or at its mechanical resonant frequency. The oscillating amplitude is used as feedback parameter to generate topography of the sample surface.[58, 59] In IC/NC AFM mode, increasing the set point value (the set point value becomes less negative) decreases the amplitude of cantilever vibration. The set point determines the oscillating amplitude (up to 100nm), which, in turn, determines tip-sample distance. The cantilever tip is set very close to or in periodical contact with the sample.[58, 60] Therefore, the tip deconvolution models for contact mode may apply to the NC-AFM mode as well. Depending on the size and geometry of the sample and the tip, deconvolution model may vary.[57, 61-63] According to the manufacturer's specification, the tip apex radius is approximately 40 nm. The dimension of IgG is about 7 nm. The large tip radius makes it possible to use the tip model of spherical shape rather than the pyramidal shape when the walls of the probe have to be taken into account.[51]

$$d_{feature} = d_{AFM}^2 / 8r_{tip} \qquad \text{(Equation 1)}$$

$d_{feature}$ – the nominal feature diameter

d_{AFM} – measured feature diameter by AFM

r_{tip} – the radius of the cantilever tip apex

After deconvolution, the calibrated diameters of the particles range from 10.2 ~ 19.5 nm. The values are in reasonable agreement with the dimension of IgGs from x-ray crystallography. The antibody density is 82 IgG molecules/μm2 on [16-mercaptohexadecanoic acid] /[11-mercapto-1-undecanol] + [16-mercaptohexadecanoic acid] = 0.1 surface. Table 2.1 presents the data of the analysis of IgG molecules in terms of measured apparent diameter, height, surface density and deconvoluted diameters for two different immobilization methods.

Table 2.1 Comparison of site-directed and random immobilization

	Height (nm)	Width (nm)	Deconvoluted width (nm)	Antibody density (IgG molecules/ μm^2)
Site-directed immobilization	3.1±0.6	71±8	14.8±4.6	82
Random immobilization	4.2±0.8	61±5	11.7±1.9	425

Periodate oxidation of antibody carbohydrate residues can be easily controlled by proper selection of reaction conditions, such as pH, temperature and periodate concentration.[52] One to eight aldehyde groups on one antibody molecule can be obtained by varying reaction parameters. In this study, since the resulting formyl group was used to immobilize antibody molecules in certain orientation, fewer antibody labeling sites were preferred. Compared to 60-80 lysines scattered across the antibody, within the same

amount of adsorption time, the scarcity of formyl groups on antibodies can explain why fewer antibodies were attached to SAMs surface, resulting in lower antibody density on surface.

Antibody orientation on surface has been an intense interest of study in recent years. A number of techniques, such as surface plasmon resonance (SPR),[64] quartz crystal microbalance (QCM),[65] ellipsometry[66] and time-of-flight secondary ion mass spectrometry (ToF-SIMS),[67] have been used to probe surface-immobilized IgG orientations.

According to crystallographic data,[56] IgG has a dimension of 14.2×8.5×3.8 nm^3 along two-fold axes, with Fab 7.0 ×5.0 ×4.0 nm^3, with Fc 8.5 ×4.5 ×3.8 nm^3. IgG is composed of three domains with two identical Fab and a Fc. The hinge region between the Fab is extremely flexible and, therefore, the prediction of the exact conformation and size is difficult for surface-immobilized IgGs. Size determination by AFM cross-section analysis in both methods showed the immobilized IgGs to be 9.8-19.5 nm in diameter and ~ 3 nm by height, which corresponds closely to IgG dimensions determined by electron microscopic measurements and x-ray diffraction.[55, 56] From the diameter and height profile data, it is speculated that in both immobilization methods IgGs were immobilized with the larger cross-section parallel to the surface. The random immobilization method does not retain most of the antibody binding activities, as shown from *in-situ* antibody-antigen binding experiment in liquid,[43] possibly due to denaturation of antibody or loss of antibody binding activity from the extensive chemical bonding between antibody and surface. In the site-directed method, the antibody is covalently attached through carbohydrate in the Fc region, which is far away from the antigen binding sites. Even if

both methods antibodies adopt the same orientation, it is expected that higher antibody binding activity should be achieved in the site-directed method, but this has not been verified experimentally. Antibody-antigen binding experiments need to be carried out to confirm the findings.

2.4 Outlook and Conclusion

In immunosensor design, high antibody surface density and proper antibody orientation are essential for biosensor sensitivity. Antibody immobilization based on SAMs on Au(111) surface showed good reproducibility. A single monolayer was formed, with no evidence of agglomeration or multilayer formation. Random antibody immobilization on mixed SAMs of 16-mercaptohexadecanoic acid and 11-mercapto-1-undecanol formed at 60°C showed slightly higher surface antibody density than that formed at room temperature. Rabbit IgGs have been immobilized on uniform SAMs surface through Fc region attachment. Non-contact mode AFM has been successfully used to image the attached antibody surface. It is speculated that antibodies on the surface adopt a parallel orientation. Further *in-situ* AFM antibody-antigen binding experiments in liquid need to be carried out to confirm the findings.

2.5 References

(1) Bundy, K. J. *Tissue Eng. Novel Delivery Sys.* **2004**, 505-520.

(2) Horiuchi, T.; Hayashi, K. *Oyo Butsuri* **2005**, *74*, 366-370.

(3) White, S. *Food Sci. Tech.* **2004**, *138*, 2133-2148.

(4) Kauffmann, J.-M. *J. Pharm. Sci.* **2003**, *28*, 107-112.

(5) Deisingh, A. K.; Thompson, M. *Can. J. Microbiol.* **2004**, *50*, 69-77.

(6) Schuhmann, W.; Habermuller, K. *New Trends Electrochem. Tech.* **2003**, *2*, 409-428.

(7) Baeumner, A. J. *Anal. Bioanal. Chem.* **2003**, *377*, 434-445.

(8) Homola, J. *Anal. Bioanal. Chem.* **2003**, *377*, 528-539.

(9) Nakamura, H.; Karube, I. *Anal. Bioanal. Chem.* **2003**, *377*, 446-468.

(10) Tamiya, E. *Mizu Kankyo Gakkaishi* **2003**, *26*, 415-420.

(11) Editor: Schena, M. *Protein microarrays*; Jones and Bartlett: Sudbury, MA, 2005.

(12) Utz, P. J.; Steinman, L.; Robinson, W. H. *Protein Microarrays* **2005**, 365-376.

(13) Wingren, C.; Montelius, L.; Borrebaeck, C. A. K. *Protein Microarrays* **2005**, 339-352.

(14) Kusnezow, W.; Pulli, T.; Witt, O.; Hoheisel, J. D. *Protein Microarrays* **2005**, 247-283.

(15) Seong, S.-y. *Protein Microarrays* **2005**, 137-157.

(16) Harwanegg, C.; Hiller, R. *Expert Rev. Mol. Diagn.* **2004**, *4*, 539-548.

(17) Yeo, D. S. Y.; Panicker, R. C.; Tan, L.-P.; Yao, S. Q. *Comb. Chem. High Throughput Screen.* **2004**, *7*, 213-221.

(18) Editor: Fung, E. T. *Protein Arrays: Methods and Protocols*; Human Press: Totowa, NJ, 2004.

(19) Krska, R.; Janotta, M. *Anal. Bioanal. Chem.* **2004**, *379*, 338-340.

(20) Varnum, S. M.; Woodbury, R. L.; Zangar, R. C. *Methods Mol. Biol.* **2004**, *264*, 161-172.

(21) Hughes, K. A. *Methods Mol. Biol.* **2004**, *264*, 111-121.

(22) Pavlickova, P.; Hug, H. *Methods Mol. Biol.* **2004**, *264*, 73-83.

(23) Gilbert, M.; Edwards, T. C.; Albala, J. S. *Methods Mol. Biol.* **2004**, *264*, 15-23.

(24) Abercrombie, D.; Allenmark, S.; Arame, S.; et al. *Affinity Chromatography: Methods*, 1988.

(25) Editor: Chaiken, I. M. *Analytical Affinity Chromatography*; CRC: Boca Raton, Fla., 1987.

(26) Dean, P. D. G.; Johnson, W. S.; Middle, F. A. *Affinity Chromatography: A Practical Approach*; IRL Press: Oxford, UK, 1985.

(27) Editors: Chaiken, I. M.; Wilchek, M.; Parikh, I. *Affinity Chromatography and Biological Recognition*; Academic Press: Orlando, Fla., 1983.

(28) Scouten, W. H. *Affinity Chromatography. Bioselective Adsorption on Inert Matrices*; John Wiley and Sons: New York, N. Y., 1981.

(29) Dunlap, R. B. *Advances in Experimental Medicine and Biology, Vol. 42: Immobilized Biochemicals and Affinity Chromatography*; Plenum: New York, N. Y., 1974.

(30) Itoyama, M.; Yabe, H.; Tanimoto, M.; Kawakami, H. In *Jpn. Kokai Tokkyo Koho*; (Fuji Spinning Co., Ltd., Japan; Snow Brand Milk Products Co., Ltd.). Jp, 1989, pp 4.

(31) Meir, W.; Talia, M. In *Israeli*; (Yeda Research and Development Ltd., Israel). Il, 1989, pp 22.

(32) Miron, T.; Wilchek, M. *J. Chromatogr.* **1981**, *215*, 55-63.

(33) Porath, J.; Caldwell, K. D. *Biotechnol. Appl. Proteins Enzymes, Pap. Conf.* **1977**, 83-102.

(34) Scouten, W. H.; Luong, J. H. T.; Brown, R. S. *Trends in Biotechnology* **1995**, *13*, 178-185.

(35) Chen, C.-H.; Tsai, T.-K. *Huaxue* **2002**, *60*, 391-397.

(36) Yamada, H. *Noncontact Atomic Force Microscopy* **2002**, 193-213.

(37) Yang, S.-R.; Ren, S.-L.; Zhang, J.-Y.; Zhang, X.-S. *Gaodeng Xuexiao Huaxue Xuebao* **2001**, *22*, 470-476.

(38) Schreiber, F. *Progress in Surface Science* **2000**, *65*, 151-256.

(39) Frederix, F.; Bonroy, K.; Laureyn, W.; Reekmans, G.; Campitelli, A.; Dehaen, W.; Maes, G. *Langmuir* **2003**, *19*, 4351-4357.

(40) Datwani, S. S.; Vijayendran, R. A.; Johnson, E.; Biondi, S. A. *Langmuir* **2004**, *20*, 4970-4976.

(41) Ostuni, E.; Grzybowski, B. A.; Mrksich, M.; Roberts, C. S.; Whitesides, G. M. *Langmuir* **2003**, *19*, 1861-1872.

(42) Patel, N.; Davies, M. C.; Hartshorne, M.; Heaton, R. J.; Roberts, C. J.; Tendler, S. J. B.; Williams, P. M. *Langmuir* **1997**, *13*, 6485-6490.

(43) Li, L.; Chen, S.; Oh, S.; Jiang, S. *Anal. Chem.* **2002**, *74*, 6017-6022.

(44) Chaki, N. K.; Vijayamohanan, K. *Biosens. Bioelectron.* **2002**, *17*, 1-12.

(45) Nelson, K. E.; Gamble, L.; Jung, L. S.; Boeckl, M. S.; Naeemi, E.; Golledge, S. L.; Sasaki, T.; Castner, D. G.; Campbell, C. T.; Stayton, P. S. *Langmuir* **2001**, *17*, 2807-2816.

(46) Chapman, R. G.; Ostuni, E.; Takayama, S.; Holmlin, R. E.; Yan, L.; Whitesides, G. M. *J. Am. Chem. Soc.* **2000**, *122*, 8303-8304.

(47) Harder, P.; Grunze, M.; Dahint, R.; Whitesides, G. M.; Laibinis, P. E. *J. Phys. Chem. B* **1998**, *102*, 426-436.

(48) Luk, Y.-Y.; Kato, M.; Mrksich, M. *Langmuir* **2000**, *16*, 9604-9608.

(49) Ostuni, E.; Chapman, R. G.; Holmlin, R. E.; Takayama, S.; Whitesides, G. M. *Langmuir* **2001**, *17*, 5605-5620.

(50) Li, L.; Chen, S.; Jiang, S. *Langmuir* **2003**, *19*, 3266-3271.

(51) Dong, Y.; Shannon, C. *Anal. Chem.* **2000**, *72*, 2371-2376.

(52) Wolfe, C. A.; Hage, D. S. *Anal. Biochem.* **1995**, *231*, 123-130.

(53) Dong, Y. Doctoral Dissertation, Auburn Univ., Auburn, AL, USA., 2001.

(54) Davies, D. R.; Sarma, V. R.; Labaw, L. W.; Silverton, E. W.; Terry, W. D. *Progr. Immunol., Int. Congr. Immunol., 1st* **1971**, 25-32.

(55) Sarma, V. R.; Davies, D. R.; Labaw, L. W.; Silverton, E. W.; Terry, W. D. *Cold Spring Harbor Symp. Quant. Biol.* **1971**, *36*, 413-419.

(56) Sarma, V. R.; Silverton, E. W.; Davies, D. R.; Terry, W. D. *J. Biol. Chem.* **1971**, *246*, 3753-3759.

(57) Xu, S.; Arnsdorf, M. F. *J. Microsc.* **1994**, *173*, 199-210.

(58) Garcia, R.; Perez, R. *Surf. Sci. Rep.* **2002**, *47*, 197-301.

(59) Takano, H.; Kenseth, J. R.; Wong, S.-S.; O'Brien, J. C.; Porter, M. D. *Chem. Rev.* **1999**, *99*, 2845-2890.

(60) Sokolov, I. Y.; Henderson, G. S.; Wicks, F. J. *Appl. Surf. Sci.* **1999**, *140*, 362-365.

(61) Xu, S.; Arnsdorf, M. F. *J. Microsc.* **1997**, *187*, 43-53.

(62) Van Cleef, M.; Holt, S. A.; Watson, G. S.; Myhra, S. *J. Microsc.* **1996**, *181*, 2-9.

(63) Keller, D. J.; Franke, F. S. *Surf. Sci.* **1993**, *294*, 409-419.

(64) Perrin, A.; Lanet, V.; Theretz, A. *Langmuir* **1997**, *13*, 2557-2563.

(65) Harteveld, J. L. N.; Nieuwenhuizen, M. S.; Wils, E. R. J. *Biosens. Bioelectron.* **1997**, *12*, 661-667.

(66) Lu, B.; Xie, J.; Lu, C.; Wu, C.; Wei, Y. *Anal. Chem.* **1995**, *67*, 83-87.

(67) Wang, H.; Castner, D. G.; Ratner, B. D.; Jiang, S. *Langmuir* **2004**, *20*, 1877-1887.

CHAPTER 3 CAPTURE ANTIBODIES IMMOBILIZED ON SELF-ASSEMBLED MONOLAYERS FOR *SALMONELLA enterica* Typhimurium DETECTION

3.1 Introduction

According to the Centers for Disease Control and Prevention (CDC), foodborne disease results in millions of human illnesses in the United States each year.[1] Among the 250 foodborne pathogens identified by CDC, *Salmonella* is the second most frequently reported cause of foodborne illness. Every year, the CDC receives reports of 40,000 cases of salmonellosis in the United States. By estimation, 1.4 million people in the US are infected, and 1,000 people die each year due to salmonellosis.[1-5]

Rapid, sensitive, cost-effective detection of *Salmonella* is, hence, crucial to food safety. Although current pathogenic bacteria detection techniques,[6-16] such as immunoassay (ELISA, RIA) or polymerase chain reaction (PCR) provide excellent detection limits, they require complex procedures and lengthy analysis time.

Biosensors have been developed for detecting environmental pollutants[17-21] and for clinical diagnosis[22, 23] in recent years. Biosensors offer rapid, sensitive, specific and cost-effective detection providing great opportunities for detection of bacteria for food safety. A biosensor is essentially comprised of the immobilization of a biomolecular recognition element on the corresponding transducer. The capture of analyte molecules

by the bioreceptor gives rise to a change in the output signal of the transducer. The change of the signal can be correlated with the concentration of analyte. Piezoimmunosensors, using a quartz piezoelectric crystal detector as the transducer, have been developed and widely used in many fields, such as the food industry[24-28] and environmental monitoring.[29-34]

The quartz crystal microbalance (QCM), based on piezoelectric detection, has been used in a number of research groups in recent years for the detection of *Salmonella*.[35-45] The efforts of *Salmonella* immunosensor development have been focused on the immobilization of antibodies on the electrode/transducer surface. In early years of immunosensor development, antibodies were immobilized onto the surface mainly through cross-linking and thiolating linking. However, due to diffusion barrier from the analyte to the transducer caused by the 3-dimensional matrix, the biosensors exhibited long response time and high detection limits. In order to achieve fast response time and lower detection limits, ordered monolayers were introduced for antibody immobilization, which entails the use of Langmuir-Blodgett (LB) film and self-assembled monolayers (SAMs). Combined with quartz crystal microbalance, immobilization of antibodies using a phospholipids monolayer produced by LB technique[43] provided a detection limit of 350±150 cells/mL and a working range of 10^2 to 10^{10} cells/mL for *Salmonella enterica* Typhimurium with a response time of less than 100 seconds. The sensitivity of the detection could be attributed to ordered monolayers and high density of antibodies on the LB film. However, the biosensor showed poor repeatability, judging from the high standard deviation value. Fung and Wong[39] developed a quartz piezoelectric crystal immunosensor for detection of *Salmonella* paratyphi. A detection limit of 1.7×10^2 cells/

mL with a response time of 50 minutes was obtained. However, with the narrow linear range of 10^2 to 10^4 cells/mL, the large percent RSD was not sufficient. Also, the coverage and distribution of bacteria on gold electrode surface was unclear.

Although the biosensors developed so far for detection of *Salmonella* Typhimurium have achieved faster response time and specific binding, biosensor sensitivity and stability still remain a great issue. In order to achieve high reproducibility, the immobilization of the bioreceptor has to be permanent and not easily displaced or removed. To achieve low detection limits, the amount of bioreceptors on or close to the surface has to be sufficient, and antibodies have to be properly oriented to bind antigens. Protein covalent immobilization techniques, which rely on the covalent bond linkage between the functional groups on the transducer surface and proteins, offer high surface protein density and low protein loss. The potential of offering high reproducibility and low detection limits has made antibody covalent immobilization desirable in immunosensor applications.

Self-assembled monolayers (SAMs) are monolayers of well-defined structural and chemical properties. In addition, the surface properties of SAMs can be controlled by adjusting the ratio and type of tail groups. By varying parameters in SAMs, protein surface density can be controlled. Ordered monolayers and the ability to control surface antibody density on self-assembled monolayers provide an ideal platform for fast detection of *Salmonella*.

In this chapter, anti-*Salmonella* IgGs are covalently immobilized on self-assembled monolayers (SAMs) through lysine groups on the antibodies. A preliminary study of immobilization through their Fc portion was conducted. The surfaces with

immobilized antibodies were subsequently exposed to high concentrations of *Salmonella enterica* Typhimurium solution. Compositions of SAMs and the use of coupling agents were investigated in order to improve viable antibody density on the SAMs surface. Scanning Electron Microscopy (SEM) was used to assess bacteria captured from solution onto antibody functionalized SAMs substrate in this work.

3.2 Experimental

Reagents and Materials. 11-Amino-undecanethiol hydrochloride was purchased from Dojindo Laboratories (Japan). Ethylamine, 2-propanol, Tween 80, (3-mercaptopropyl)trimethoxysliane (MPS), 3-mercaptopropyloic acid, 11-mercapto-1-undecanoic acid, thioctic acid and butanethiol were obtained from Aldrich Chemical Company and used as received. Glass microscope slides, sodium periodate, ammonium hydroxide were obtained from Fisher Scientific. Micron microfilters were purchased from Microns.

Affinity Chromatography purified rabbit anti-*Salmonella* IgG "Tiffy" (30 mg/mL) and *Salmonella enterica* Typhimurium solution (10^9 colony forming unit/mL) were provided by Dr. Huang from the Department of Nutrition and Food Science at Auburn University.

Substrate Preparation. Substrate was prepared by silanization of glass microscope slides, followed by sputter coating a layer of gold on the glass. Microscope slides were cut to 0.5 × 0.5 cm^2 glass squares. The glass squares were silanized according to procedures described in the literature.[46] Prior to chemical modification, all glass slides were treated with Piranha solution. 2.5g MPS, 2.5g H_2O, 100g 2-propanol and the glass

squares were heated to reflux for 10 minutes. The glass squares were then rinsed with 2-propanol. Subsequently, they were heated in the oven at 100-105°C for 3 cycles. Finally, they were rinsed with DI water.

The gold layers were deposited by sputter coating on a Pelco SC-7 Auto Sputter Coater with a 99.99% gold plate. Sputter coating parameters: working distance 5 cm, 0.08 mbar, 120 seconds. Estimated thickness was 114 nm from the sputter coating calibration chart. The Au layers showed robustness, withstanding delamination in water.

Agglutination test. Prior to antibody immobilization, antibody reactivity was checked against *S. enterica* Typhimurium by a slide agglutination test. *S. enterica* Typhimurium agglutinated in the presence of the specific antibody "Tiffy".

Control experiment. Control experiments were performed to test physical adsorption of *Salmonella* on different SAMs surfaces. Briefly, after formation, SAMs were exposed to 10^9 colony forming unit (CFU)/mL *Salmonella* PBS solution for 2 hrs. After samples were gently washed with water, fixed, and sputter coated, they were examined by SEM.

Antibody solution reconstitution. The original "Tiffy" solution consists of: 100 mM Tris, 2 mM $MgCl_2$, 20 mM glycine, 30 mM sodium azide, pH 8.0, with IgG concentration 30 mg/mL. To reconstitute the antibody solution, 18.5 μL of 30 mg/mL "Tiffy" was diluted in 0.5 mL PBS buffer (10mM, pH 7.3). The solution was filtered with a Micron-50 microfilter device at 3000×g and reconstituted to 1 mg/mL with an appropriate buffer.

Antibody oxidation. Antibody oxidation was carried out according to the procedure described in the literature.[47] Briefly, 50 μL of 1 mg/mL antibodies solution

was added into 50 μL of 20mM fresh sodium periodate solution at 0°C. After 20 minutes in dark, the mixed solution was quenched with glycerol. The solution was filtered by Microcon-50 microfilter at 3000 × g, and reconstituted to 5 μg/mL with PBS.

SAMs Preparation. SAMs were formed by immersing gold samples in 1mM alkanethiol or mixed organothiol ethanol solution for 24 hrs at room temperature. NH_2-terminated SAMs were formed by immersing gold coated glass squares in 1mM 11-amino-undecanethiol/10% ammonium hydroxide (v/v) ethanol solution for 24 h. The SAMs were rinsed sequentially with pure ethanol, 10% acetic acid, and ethanol and dried in a N_2 stream. Prior to further chemical modification, the glass squares were thoroughly rinsed with ethanol and DI H_2O to wash away loosely bound thiols on surfaces.

Covalent Immobilization of rabbit IgG. For the random immobilization, carboxyl groups of the SAMs on the glass squares were activated with 15 mM NHS and 75 mM EDC for 30 min.[39, 48] Then, samples were rinsed with H_2O, ethanol and H_2O. Subsequently, the samples were incubated in 5 μg/mL rabbit anti-*Salmonella* antibody solution in PBS (10 mM pH 7.3). After removed from the solutions, the samples were first washed with water, then with 1% Tween 80 for 1 min and finally rinsed with water. Then, all the samples were put in 2% ethylamine/H_2O solution for 1 hr. Prior to use, the functionalized glass squares were washed with DI water and dried under a stream of nitrogen.

In the Fc immobilization experiment, antibodies were immobilized by exposing the NH_2-terminated SAMs to 5 μg/mL oxidized antibody in 10 mM PBS (pH 6.0) for 6 hrs. Prior to use, the functionalized glass were washed with DI water, dried under a stream of nitrogen.

Antibody-antigen binding. Prior to applying to the antibody bound surface, *Salmonella* solution in a centrifuge tube was vortexed for 5 min. Then, the samples were immersed in *Salmonella* solution (10^9 CFU/mL) for 2 hrs with the gold-coated surface facing up. After removed from the solution, the glass squares were gently rinsed with DI water.

Cell fixation and sputter coating. Before being examined by SEM, the bacteria coated surface needed to be fixed and coated with Au. The bacteria were fixed in the following procedure: samples were placed in a tilted Petri dish with about 2 mL 2% aqueous solution of osmium tetraoxide. The Petri dish was covered to avoid evaporation and allowed to sit for 4 hours. The osmium tetraoxide solution was removed using a transfer pipet. The samples were placed on a new Petri dish and allowed to dry for 30 minutes. The samples were then placed on the sample table and sputter coated with 99.99% gold target. (Sputter current=40mA; Coating time: 120 sec; Argon leak pressure: 0.08 mbar; Working distance: 5 cm.) The samples were then mounted onto aluminum stubs by using conductive double-stick carbon tape before SEM imaging.

Characterization of *Salmonella enterica* Typhimurium on gold surface. All samples were imaged at 10 kV on a Zeiss DSM 940 Scanning Electron Microscope with digital imaging located in the Department of Biological Sciences at Auburn University.

3.3 Results and Discussion

Immobilization of anti-*Salmonella* IgG on SAMs. AFM measurement of glass slides showed a flat, featureless surface. After gold deposition, ca. 4 nm gold particles

were seen deposited onto the glass (image not shown). Under SEM, the gold coated glass substrate exhibited a featureless surface.

Antibodies were immobilized covalently onto Au substrate, linked by SAMs. Antibody concentration was usually kept low to minimize non-specific adsorption. Before the antibody was immobilized onto the SAMs surface, it was necessary to examine the composition of the antibody solution. In random antibody immobilization, the antibody was immobilized through the amino groups on lysine. However, both Tris and glycine, as well as the preservative azide, as part of the buffer, contain amino groups and can act as nucleophiles for the active intermediate of EDC or EDC/NHS. In addition, compared to concentration of amino groups of lysine on antibody molecules, the amine concentration in the buffer was much greater than that on antibodies. If immobilization was performed with antibody in the original buffer, even after dispension, Tris and glycine would compete with antibodies for the NHS intermediate. The result would be that no antibodies would covalently bond to SAMs. Any antibody on the surface would result from non-specific adsorption. Hence, it is essential that prior to immobilization, the antibody solution be reconstituted by either dialysis or filtering to remove Tris, glycine and azide. The reconstitution in this experiment consisted of filtration with a micron-50 microfilter device. Only molecules larger than 50 kDa were retained after filtration.

After the antibody solution was reconstituted, it was applied to an EDC/NHS activated surface. Phosphate buffer saline, or PBS, was usually used to dispense the antibody solution. However, when directly using EDC to activate the carboxylic acid groups, PBS should be avoided. The incompatibility of EDC and PBS may account for the poor performance of a previous *Salmonella* piezoimmunosensor.[45]

For quartz piezoelectric crystal microbalance, the binding events occur on a polycrystalline gold electrode surface. Therefore, in this work polycrystalline gold surface was used as the substrate for immobilization of antibodies and the capture of bacteria. Since the Au substrate is rough compared to the small dimension of IgGs as well as the large dimension of a *Salmonella enterica* Typhimurium cell, it is not feasible to image antibody molecules or binding events on a surface with AFM, which usually scans smooth surfaces and areas up to 100 μm. Rather, the binding activities of IgGs were examined by performing a bacteria assay, which will be discussed shortly.

Physical adsorption. Control experiments were performed to examine bacteria adhesion to surfaces. In biosensor development, non-specific interaction of analyte with surfaces should be minimized, if possible. Otherwise, non-specific adsorption will interfere with data interpretation, such as the frequency changes for QCM. Through SEM examination, it was found the *Salmonella enterica* Typhimurium bacteria did not adsorb to bare gold surface or SAMs surface (including thioctic acid, butanethiol and amino-terminated monolayer). Exposing bare gold surfaces to *S. enterica* Typhimurium solution resulted in a flat, featureless surface (Figure 3.1). After butanethiol monolayers surfaces were directly exposed antibody solution, however, some bacteria cells did adsorb to surface, which means antibodies were adsorbed to surface non-specifically (Figure 3.2). However, the non-specifically adsorbed bacteria density is low overall, compared to antibody binding bacteria. For example, for SAMs surface of thioctic acid ratio of 0.4, the non-specific adsorption accounted for about 3% of the captured bacteria (refer to Table 3.1 for calculation). It has to be pointed out that this observation only applies to *Salmonella enterica* Typhimurium and the inspected surfaces. A wide range of SAMs

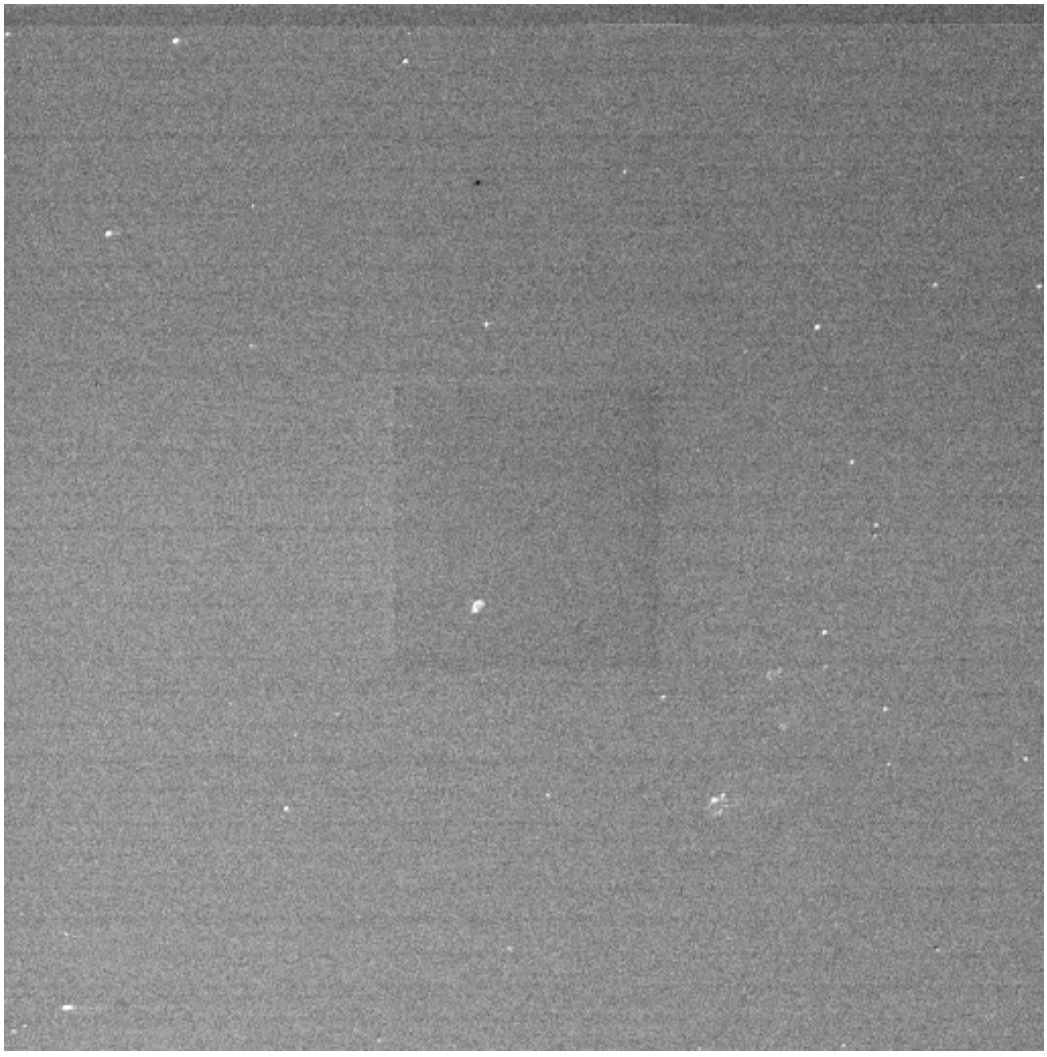

Figure 3.1 Control experiment: SEM image (500×) of captured *Salmonella enterica* Typhimurium on butanethiol SAMs.

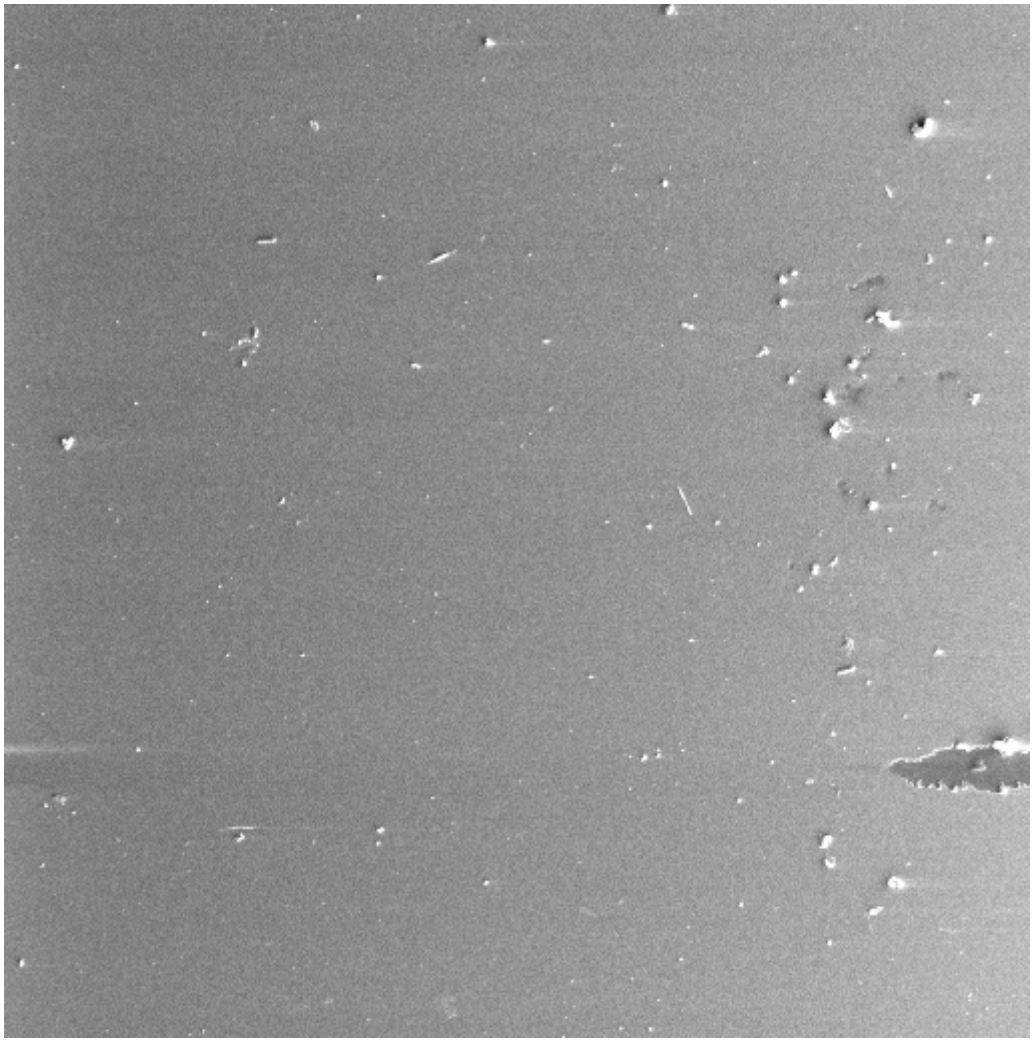

Figure 3.2 Control experiment: SEM image (500×) of captured *Salmonella enterica* Typhimurium on butanethiol SAMs pretreated with anti-*Salmonella* antibody solution

Table 3.1 *S. enterica* Typhimurium density on SAMs and SAMs composition

SAMs composition	[TA]/[TA]+[BT] in solution					Pure 3-MPA	[3-MPA] / [11-MUA] =10:1	Site-directed method
	0	0.1	0.4	0.8	1			
Number of clusters	7 ± 2	37 ± 8	52 ± 10	148 ± 16	592 ± 30	576 ± 32	768 ± 56	242 ± 14
Average cluster size	1	2.5	4.0	5.3	4.1	4.2	1.7	2.1
Bacteria density* ($\times 10^5$ cells/cm^2)	0.22 ± 0.06	2.98 ± 0.64	6.72 ± 1.29	25.3 ± 2.7	78.3 ± 4.0	78.0 ± 4.3	42.1 ± 3.1	16.4 ± 1.0

*Sample calculation of bacteria density for pure thioctic acid SAMs based on 500× SEM micrographs:

Field of view 176 μm × 176 μm = 3.1×10^{4} μm^2 = 3.1×10^{-4} cm^2

Average number of clusters in each grid: 37

Total number of clusters: 37 × 16 = 592

Total number of bacteria: 592 × 4.1= 2427.2

Density of *S. enterica* Typhimurium 2427.2 / 3.1×10^{-4} cm^2 = 7.83×10^{6} / cm^2

have been selected as model surface systems to test for bacteria adhesion because SAMs allow molecular-level control of surface properties. Studies have shown different bacteria have different bacteria adhesion capacities on even the same SAMs surfaces.[49] Therefore, the bacteria adhesion capacity does not apply to other bacteria such as *E.Coli*.

Bacteria assays. Previously published research on *Salmonella* immunosensors did not reveal *Salmonella* coverage and distribution on surfaces. To ensure the repeatability of the detection of *Salmonella enterica* Typhimurium, the gold electrode surfaces were monitored. For a quartz piezoelectric crystal immunosensor, frequency change is directly related to the mass change on the gold electrode surface according to the Sauerbrey equation, which in turn related to the amount of bacteria on surface. Therefore, before QCM frequency study, it is necessary to examine the bacteria on the gold electrode surface in detail. The dimension of *Salmonella* cells range from one to six μm. Scanning electron microscopy is a suitable tool to examine the surface topography of bacteria captured surface. The advantage of this approach is that direct interrogation of physical features of captured bacteria on substrate is made possible. In addition, since antibody concentration on surface can be controlled by varying SAMs composition ratios, the effect of SAMs composition ratio on bacteria density on SAM surfaces was also studied.

After antibodies were immobilized onto SAMs on Au substrate, the substrate was exposed to *Salmonella enterica* Typhimurium solution. The captured bacteria on the substrates were subsequently imaged by SEM. Figure 3.3 - 3.6 are SEM images of captured *S. enterica* Typhimurium on the substrate after incubating immobilized IgGs on SAMs of different compositions in a solution of *S. enterica* Typhimurium at a

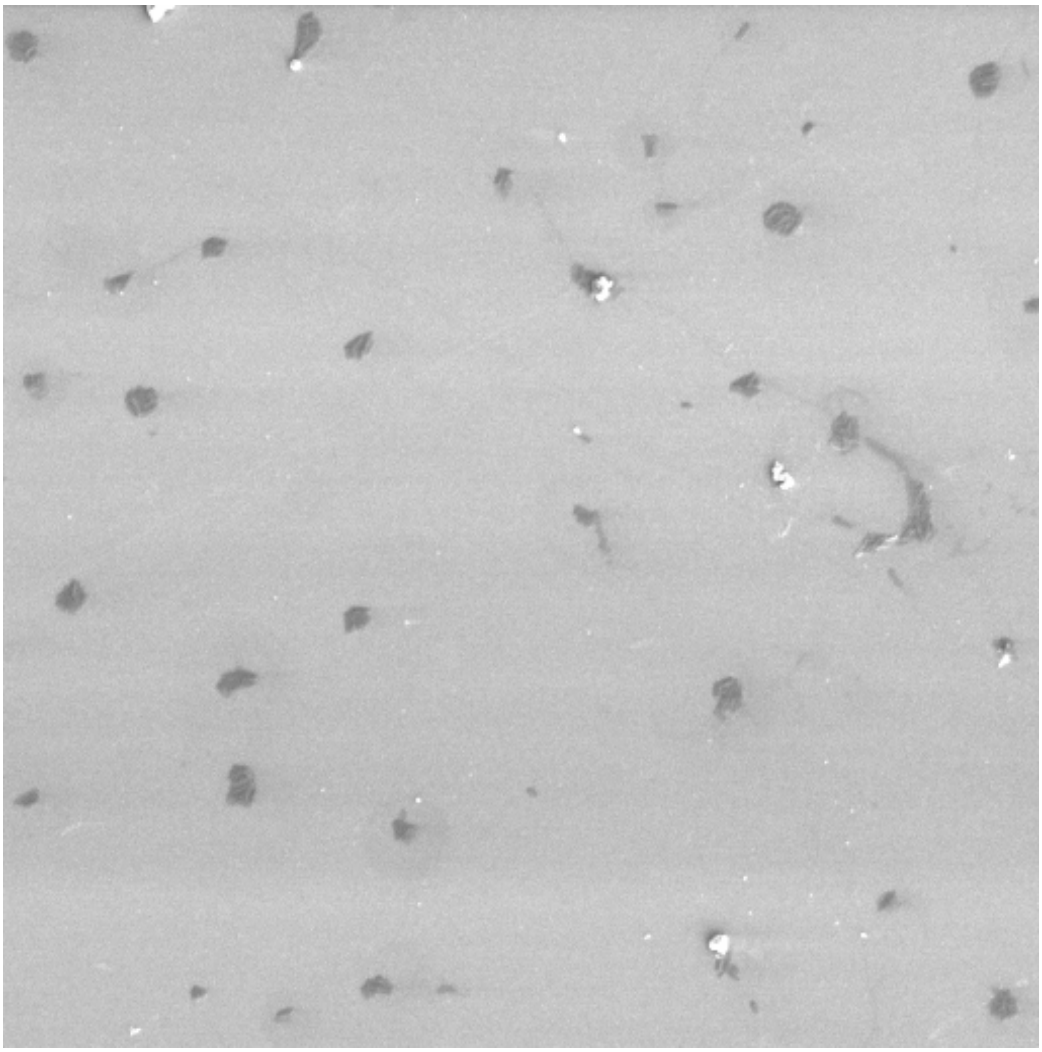

Figure 3.3 SEM image (500×, 176 μm) of captured *Salmonella enterica* Typhimurium on mixed SAMs. [TA]/[TA]+[BT] = 0.1

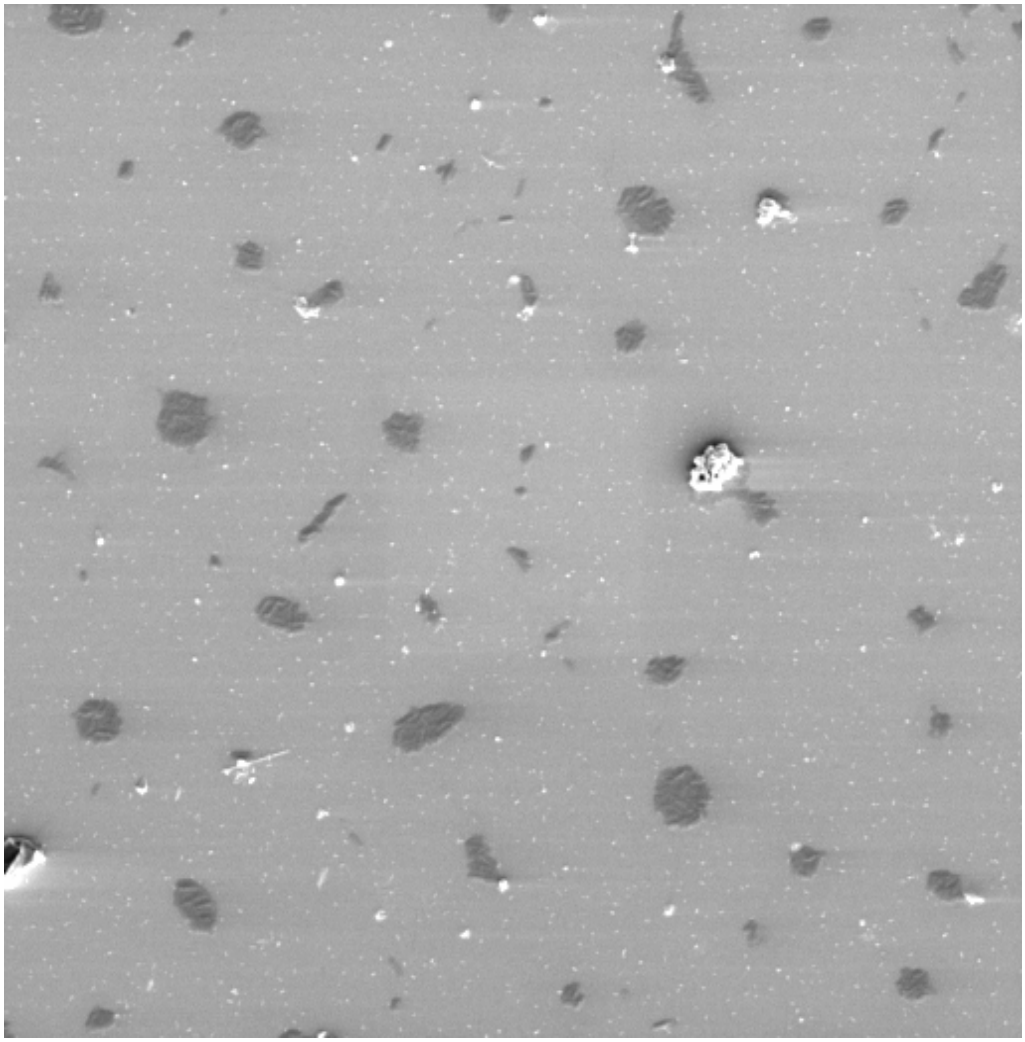

Figure 3.4 SEM image (500×) of captured *Salmonella enterica* Typhimurium on mixed SAMs. [TA]/[TA]+[BT] = 0.4

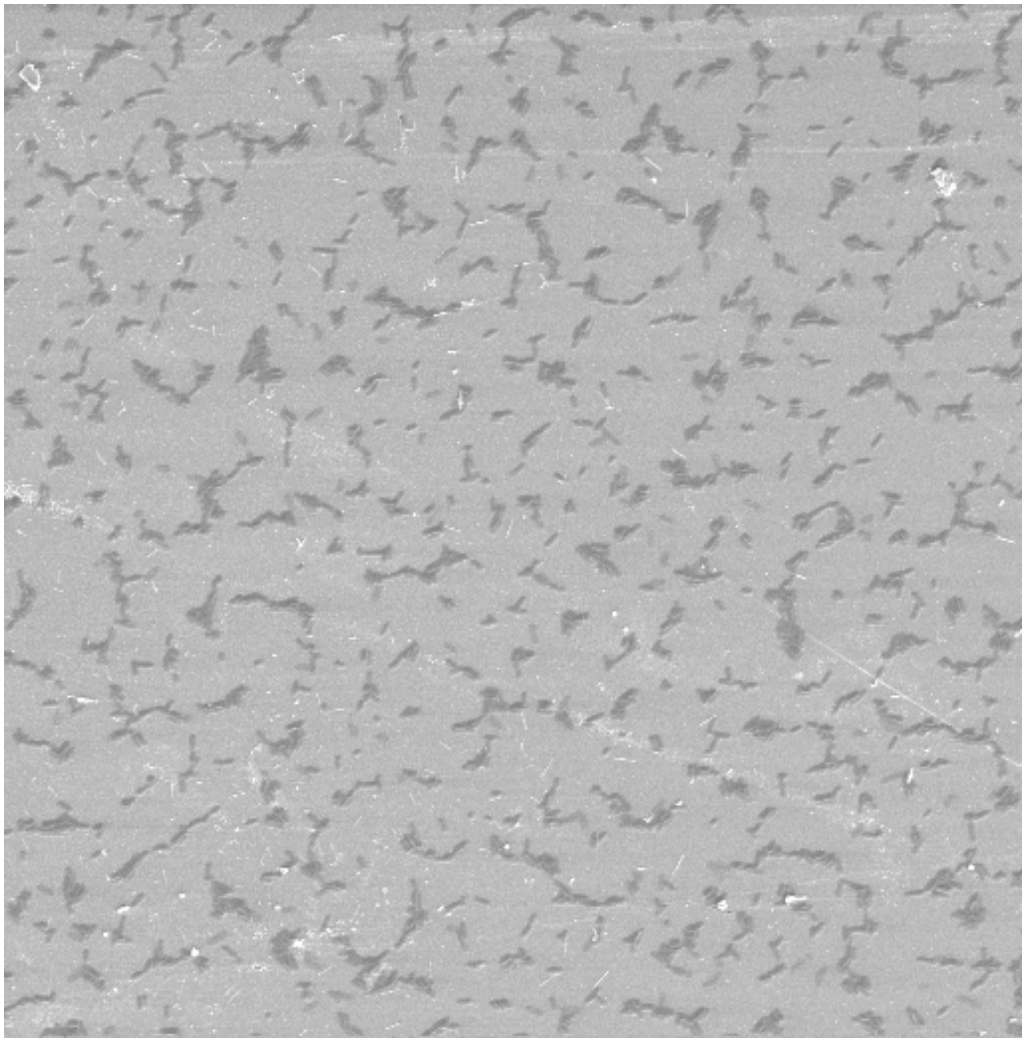

Figure 3.5 SEM image (500×) of captured *Salmonella enterica* Typhimurium on 3-mercaptopropanoic acid SAMs

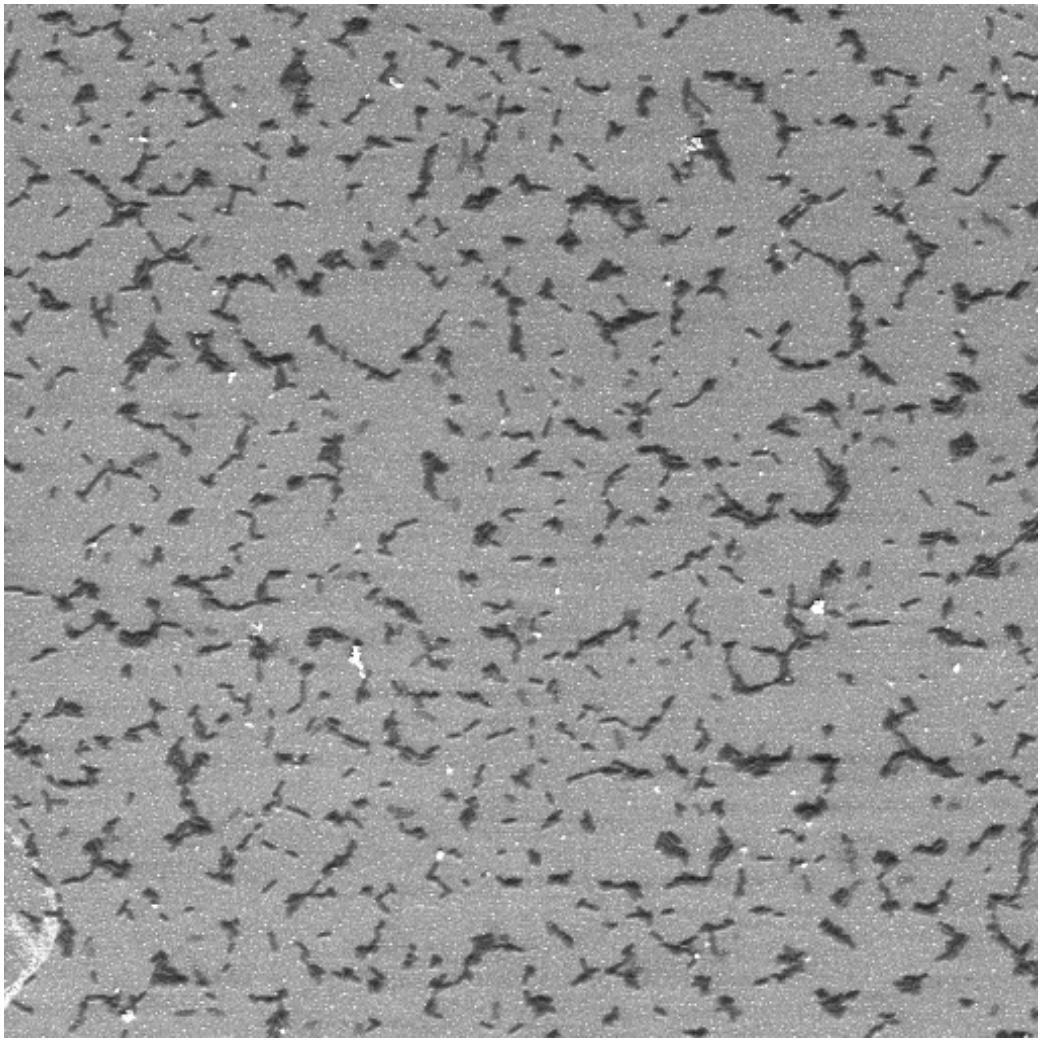

Figure 3.6 SEM image (500×) of captured *Salmonella enterica* Typhimurium on pure thioctic acid SAMs

concentration of 10^9 cells/mL. For image analysis, 500 × magnification was used so that individual bacterium can be distinguished in the images. When imaged at lower magnification, more bacteria cells are found in the field of view than at larger magnification.

Carboxylate-terminated and methyl-terminated mixed SAMs are the most popular mixed SAMs. Mixed SAMs of thioctic acid and butanethiol have been studied in detail in our research group[50] and were thus selected as the platform for immobilization of antibodies in this study.

Figure 3.3 and 3.4 are the SEM images when solution thioctic acid concentration ratios of 0.1 and 0.4 are used to prepare the SAMs. When compared with the butanethiol control experiment, it can be seen that these objects have a tendency to selectively bind to immobilized antibody regions on the surfaces. The SEM images show that a higher ratio of carboxylic acid on mixed SAMs resulted in a higher density of captured *S. enterica* Typhimurium on substrate surface.

To quantify *S. enterica* Typhimurium on SAMs, a grid system superimposed on 500× SEM micrographs were used to conduct point counting. Figure 3.7 is an example of the point counting of Figure 3.6, showing an overlay of the grid system. Point counting by hand yielded an average cluster number of 37 per grid. The point counting procedure confirmed that the bacteria are distributed evenly on SAM surfaces, and immobilization of protein by covalent bonding produced a highly uniform surface for capturing *S. enterica* Typhimurium. SAMs composition, the corresponding number of bacteria colonies, and bacteria density were illustrated in Table 3.1. A sample calculation of bacteria density was also shown. Figure 3.8 shows a correlation of the amount of

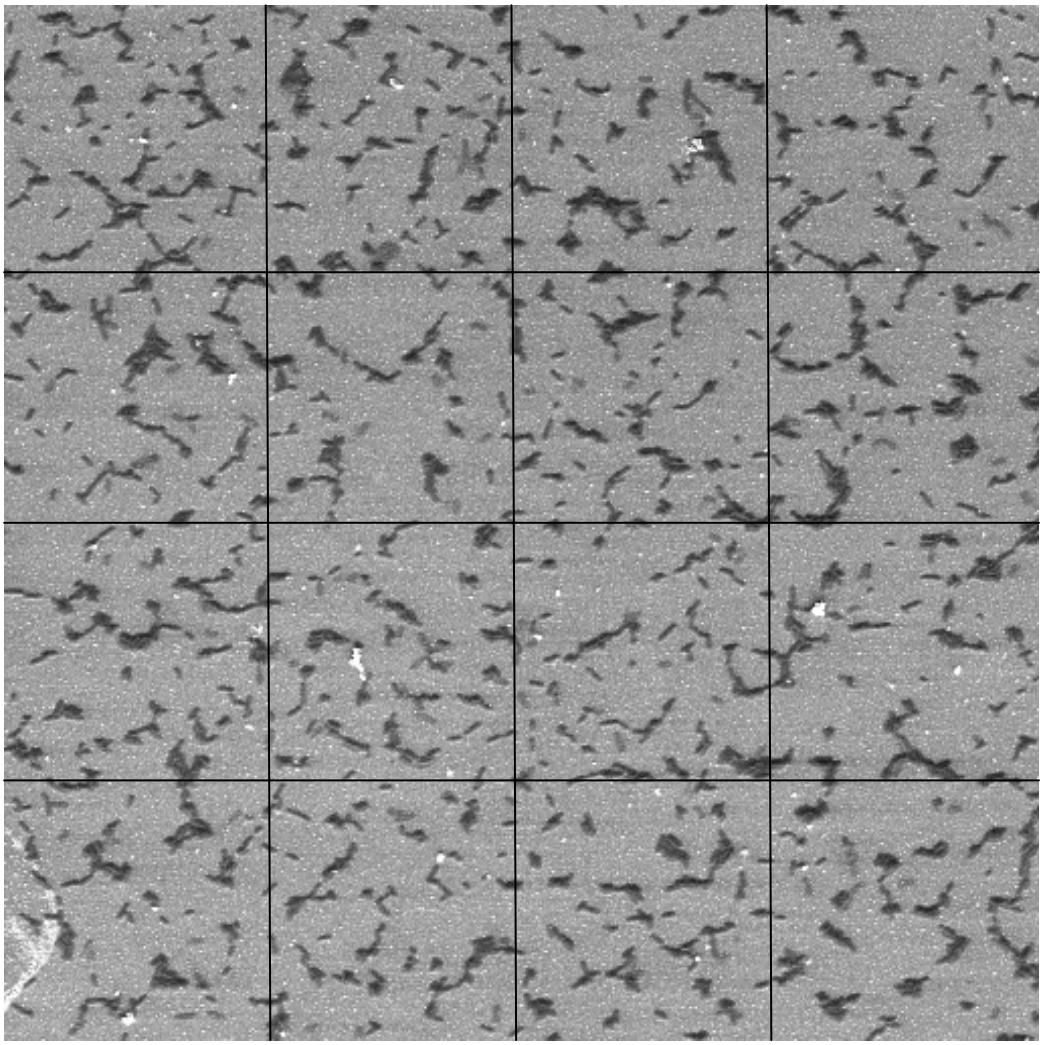

Figure 3.7 SEM image (500×) of captured *Salmonella enterica* Typhimurium on pure thioctic acid SAMs with overlay of a grid system shown for point counting

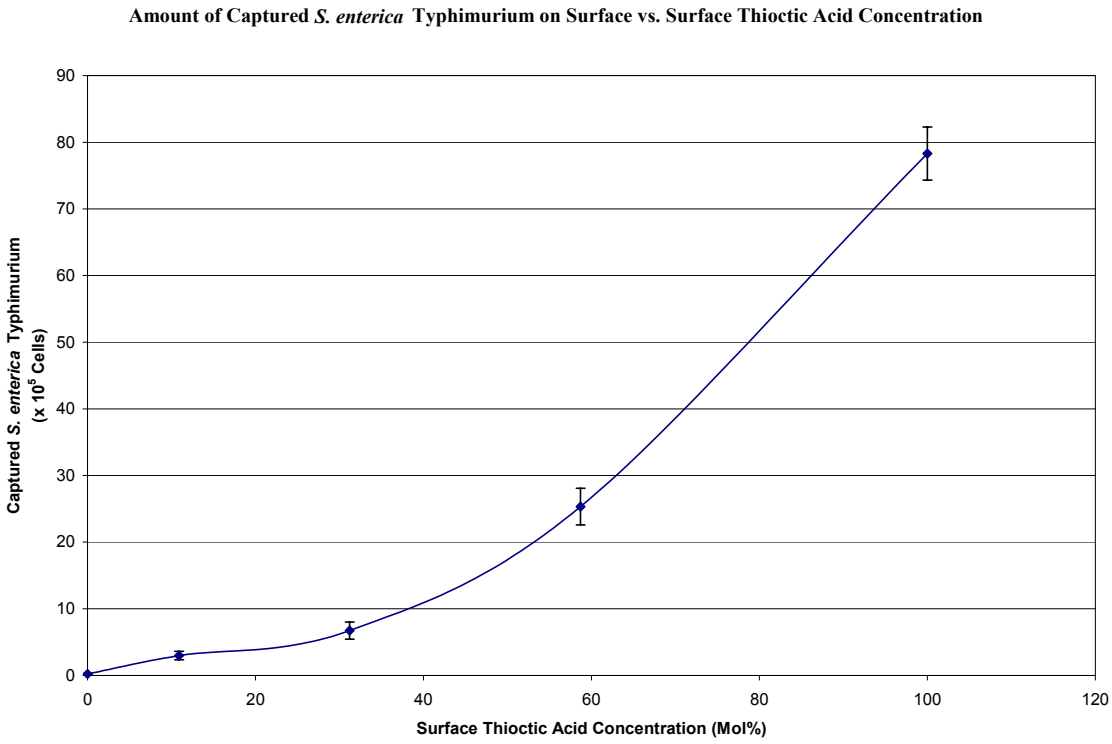

Figure 3.8 Number of captured *S. enterica* Typhimurium cells on surface as a function of surface thioctic acid concentration

captured *S. enterica* Typhimurium as a function of the thioctic acid concentration on SAMs based on Table 3.1. It can be seen from the graph that the number of bacteria on the gold surfaces increases as the surface thioctic acid concentration increases. The bacteria density on the surface reaches a maximum of 7.83×10^6 cells/ cm^2 when thioctic acid is the sole component on SAMs.

Figure 3.5 and 3.6 are the SEM images of captured *S. enterica* Typhimurium on pure 3-mercaptopropanoic acid and pure thioctic acid SAMs. The two images are comparable in bacteria density and coverage (7.83×10^6 cells/ cm^2 and 7.80×10^6 cells/ cm^2, respectively). Although two different organothiols were used for formation of SAMs, they resulted in almost the same bacteria coverage. This can be attributed to the same carboxylate group density on SAMs surface when pure thioctic acid and 3-mercaptopropanoic acid were used to form the monolayers.

Figure 3.9 is a 500× SEM image of a surface of antibodies immobilized on mixed carboxylate-terminated SAMs of 3-mercaptopropyloic acid (3-MPA) and 11-mercapto-1-undecanoic acid (11-MUA) after incubation in a solution of *S. enterica* Typhimurium at a concentration of 10^9 cells/mL. In Figure 3.9, the surface shows slightly higher number of clusters of captured *S. enterica* Typhimurium than that on pure 3-MPA SAMs, but lower bacteria density, 4.21×10^6 cells/ cm^2 compared to 7.80×10^6 cells / cm^2. SPR and AFM showed[48] immobilization of protein onto mixed carboxylate-terminated self-assembled monolayers resulted in increased coverage of proteins, compared with homogenous SAMs. Protein coverage was found to be higher in the order of 3-MPA, 11-MUA, and mixed SAMs, respectively. More accessible carboxylate groups on mixed carboxylate-

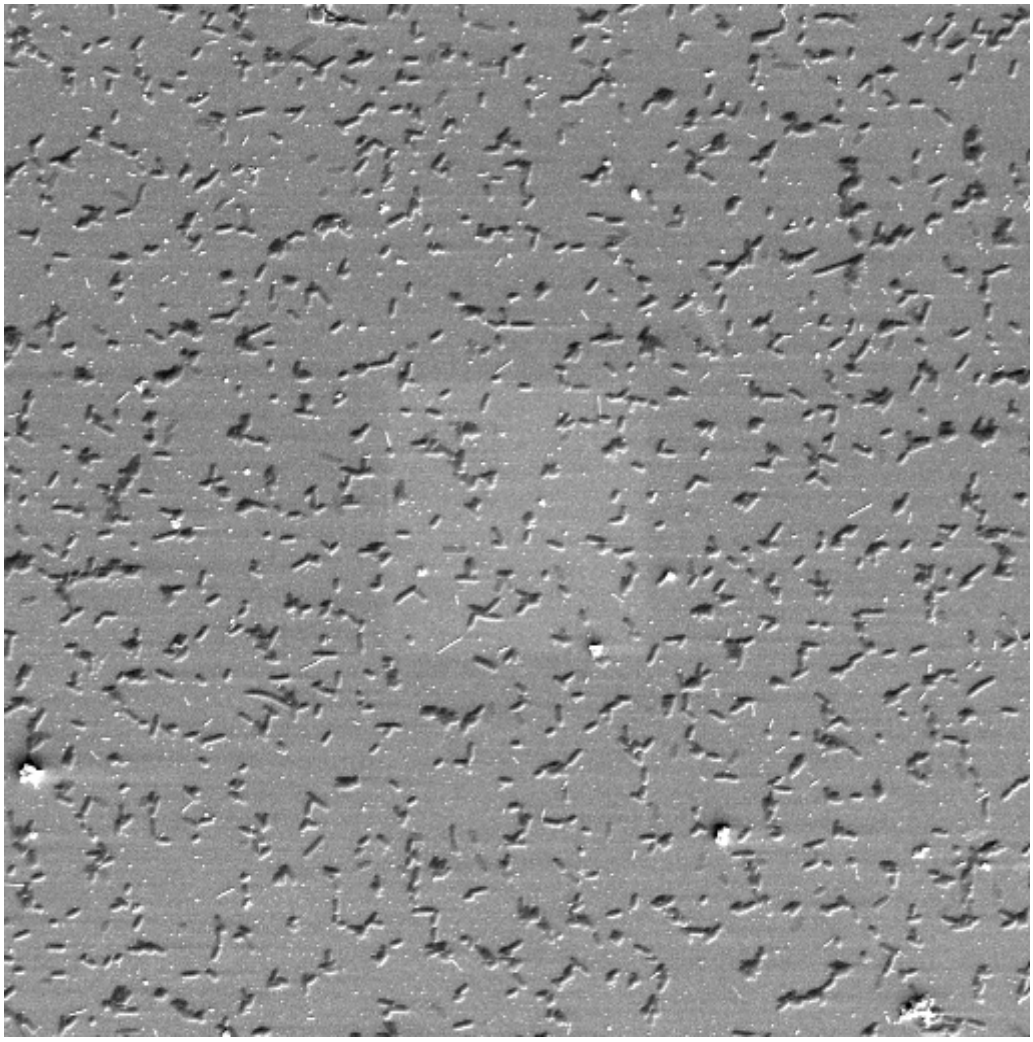

Figure 3.9 SEM image (500×) of captured *Salmonella enterica* Typhimurium on mixed SAMs. [3-MPA]/[11-MUA]=10/1

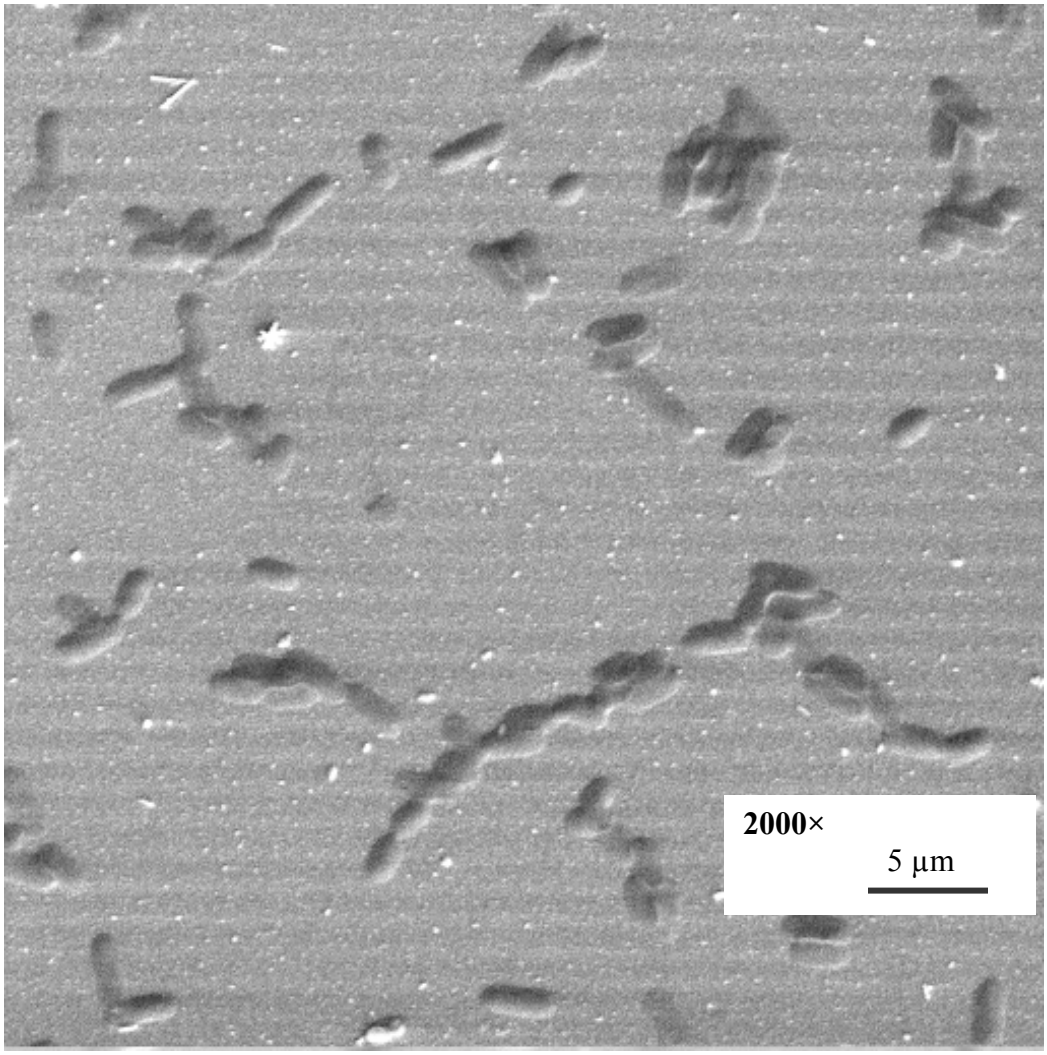

Figure 3.10 SEM image (2000×) of captured *Salmonella enterica* Typhimurium on mixed SAMs. [3-MPA]/[11-MUA]=10/1

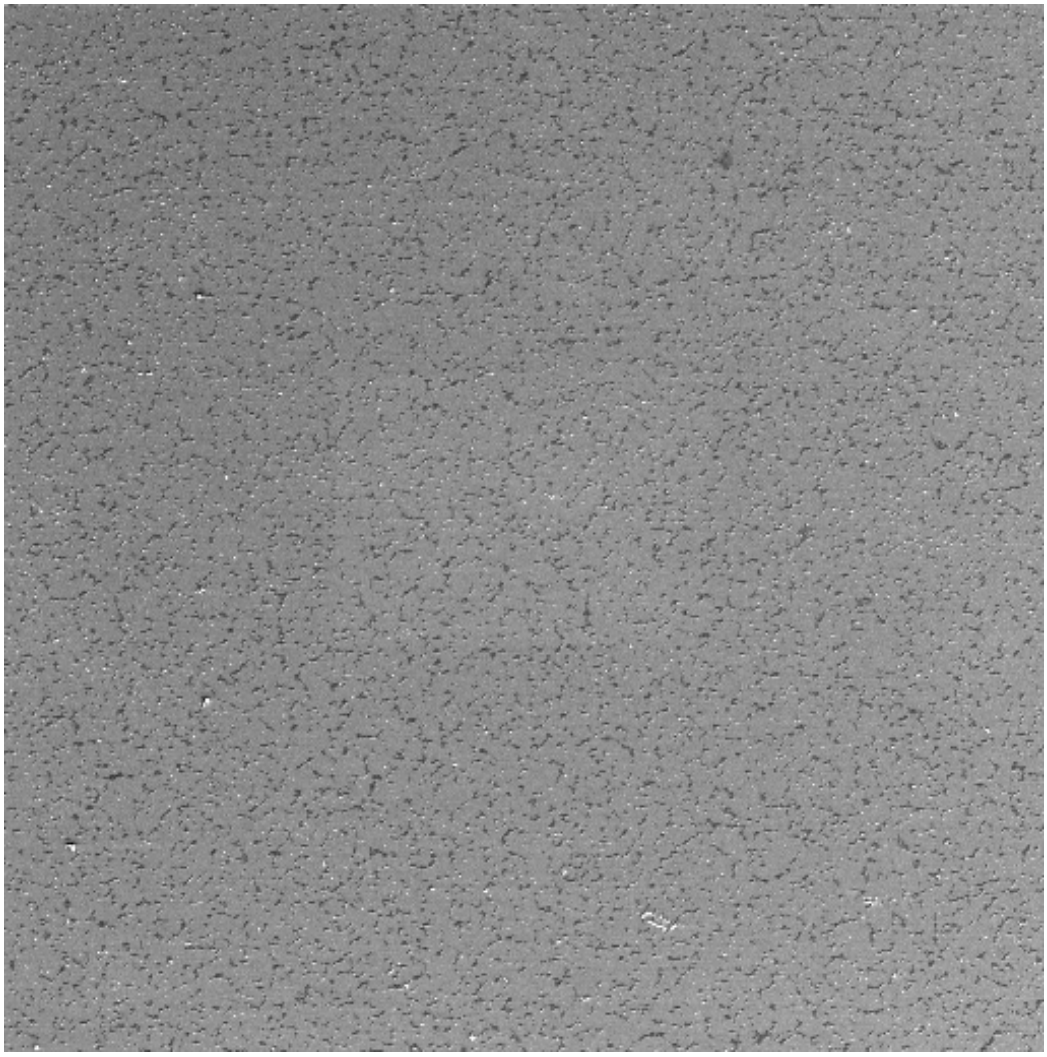

Figure 3.11 SEM image (120×) of captured *Salmonella enterica* Typhimurium on mixed SAMs. [3-MPA]/[11-MUA]=10/1

terminated SAMs did not resulted in higher *Salmonella* coverage, possibly due to the random nature of the antibody immobilization method.

Figure 3.10 is an image of higher magnification of the sample in Figure 3.9. The 2000× SEM image clearly shows the presence of rod-shaped objects with 1-6μm in length and 1μm in width distributed on the surface. These are *S. enterica* Typhimurium cells. The image also shows that the bacterial cells on the surface have a tendency to be aggregated together. It is unclear at this point whether the aggregates of *S. enterica* Typhimurium cells on the surfaces were due to the high concentration of bacteria solution the surface was exposed to. Small, white particles are salt particles from the buffer that deposited on the surface. The same sample was also imaged at a lower magnification 120× in Figure 3.11. The dimension of the image is 736×736 μm^2. This images shows the bacteria are distributed uniformly, covering the whole substrate surface.

To achieve higher surface coverage of *S. enterica* Typhimurium on mixed SAMs substrate prompted adopting a different antibody immobilization approach. Immobilization through the carbohydrate at IgG Fc portion was chosen because the antibody Fc portion is far from the antibody binding site, and it was hoped to preserve antibody binding activity after immobilization. 11-amino-undecanethiol SAMs were selected to link the aldehyde groups on oxidized antibodies to the SAMs surface. Figure 3.12 is a 500× SEM image of a surface of oxidized antibody immobilized on 11-amino-undecanethiol SAMs after incubation in a solution of *S. enterica* Typhimurium at a concentration of 10^9 cells/mL. The surface yielded a bacteria density of 1.64×10^6 cells/ cm^2. Control experiments showed that *S. enterica* Typhimurium did not adhere to 11-amino-undecanethiol SAMs surface (image not shown). So it can be concluded that the

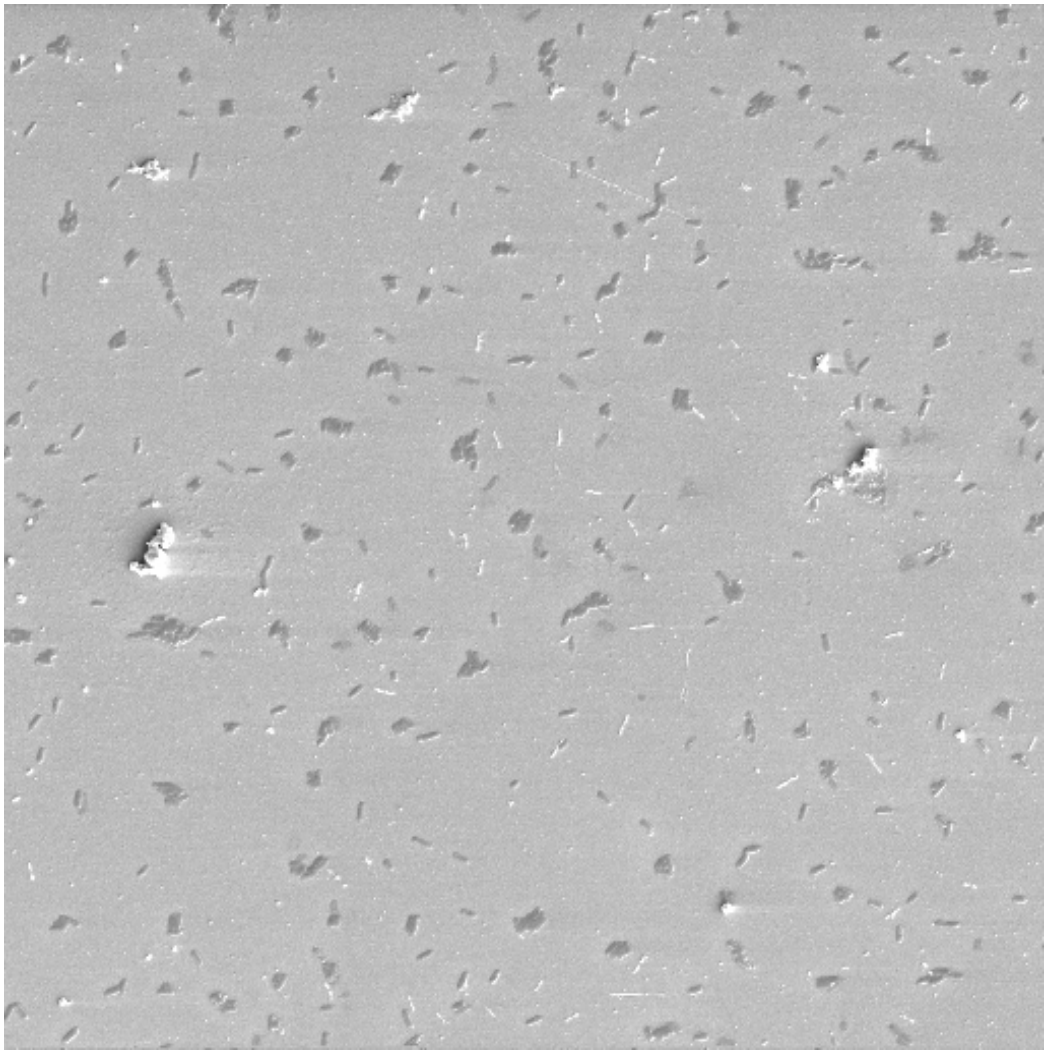

Figure 3.12 SEM image (500×) of captured *Salmonella enterica* Typhimurium on 11-amino-undecanethiol monolayers

captured bacteria were bound to immobilized antibody regions on the substrate selectively. According to the study in Chapter 2, antibodies possibly adopted a parallel orientation on the surface when immobilized through carbohydrate in the Fc portion. Although compared with Figure 3.6, bacteria density (1.64×10^6 cells/ cm^2) was not as large as when using thioctic acid pure monolayer and the random immobilization method (7.83×10^6 cells / cm^2). Optimization of reaction conditions, such as the selection of SAMs, immobilization pH, and the effect of $Na(CN)BH_3$ as the reduction agent, may lead to higher bacteria surface coverage. Other antibody immobilization methods that are capable of controlling antibody orientations, such as immobilization through protein A or IgG $(Fab')_2$ should also be considered to achieve better bacteria density on surfaces.

3.4 Conclusion

Rabbit anti-*Salmonella* IgGs were covalently immobilized on pure or mixed SAMs surfaces, and the antibody functionalized surfaces were capable of detecting *Salmonella enterica* Typhimurium in PBS solution. The surfaces of captured bacteria and bacteria coverages were examined by SEM. The random antibody immobilization approach provided highly uniform and partial surface bacteria coverage when exposed to high concentration of *Salmonella enterica* Typhimurium solution. Pure thioctic acid SAMs provided the best bacteria coverage of 7.83×10^6 cells/ cm^2 amongst all the SAMs tested. A preliminary study of the efficacy of site-directed antibody immobilization on detection of *Salmonella enterica* Typhimurium was carried out, and a bacteria density of 1.64×10^6 cells / cm^2 was achieved. Further optimization of the experimental conditions of site-directed method is needed in order to provide higher bacteria density on gold

surfaces. The reported SAMs based protein immobilization provides a generic platform of bioreceptor immobilization in biosensor development which can be tailored for detection of *Salmonella enterica* Typhimurium and a variety of other foodborne pathogens.

3.5 Acknowledgement

The author thanks Dr. Tung-Shi Huang from the Department of Nutrition and Food Science at Auburn University for providing anti-*Salmonella* IgGs and *Salmonella enterica* Typhimurium PBS solutions.

3.6 References

(1) Mead, P. S.; Slutsker, L.; Dietz, V.; McCaig, L. F.; Bresee, J. S.; Shapiro, C.; Griffin, P. M.; Tauxe, R. V. *Emerg. Infect. Dis.* **1999**, *5*, 607-625.

(2) Altekruse, S. F.; Cohen, M. L.; Swerdlow, D. L. *Emerg. Infect. Dis.* **1997**, *3*, 285-293.

(3) Olsen Sonja, J.; Ying, M.; Davis Meghan, F.; Deasy, M.; Holland, B.; Iampietro, L.; Baysinger, C. M.; Sassano, F.; Polk Lewis, D.; Gormley, B.; Hung Mary, J.; Pilot, K.; Orsini, M.; Van Duyne, S.; Rankin, S.; Genese, C.; Bresnitz Eddy, A.; Smucker, J.; Moll, M.; Sobel, J. *Emerg. Infect. Dis.* **2004**, *10*, 932-935.

(4) Wallace, D. J.; Van Gilder, T.; Shallow, S.; Fiorentino, T.; Segler, S. D.; Smith, K. E.; Shiferaw, B.; Etzel, R.; Garthright, W. E.; Angulo, F. J. *J. Food Prot.* **2000**, *63*, 807-809.

(5) Varma Jay, K.; Molbak, K.; Barrett Timothy, J.; Beebe James, L.; Jones Timothy, F.; Rabatsky-Ehr, T.; Smith Kirk, E.; Vugia Duc, J.; Chang Hwa-Gan, H.; Angulo Frederick, J. *J. Infect. Dis.* **2005**, *191*, 554-561.

(6) Vazquez-Novelle, M. D.; Pazos, A. J.; Abad, M.; Sanchez, J. L.; Perez-Paralle, M. L. *FEMS Microbiol. Lett.* **2005**, *243*, 279-283.

(7) Saxena, M. K.; Singh, V. P.; Lackchura, B. D.; Saxena, A.; Sharma, B. *Indian Journal of Biotechnology* **2004**, *3*, 37-40.

(8) Cheung, P. Y.; Chan, C. W.; Wong, W.; Cheung, T. L.; Kam, K. M. *Lett. Appl. Microbiol.* **2004**, *39*, 509-515.

(9) Jolley, M. E.; Nasir, M. S. In *U.S. Pat. Appl. Publ.*; (USA). Us, 2004, 12 pp.

(10) Ellingson, J. L. E.; Anderson, J. L.; Carlson, S. A.; Sharma, V. K. *Mol. Cell. Probes* **2004**, *18*, 51-57.

(11) Uyttendaele, M.; Vanwildemeersch, K.; Debevere, J. *Lett. Appl. Microbiol.* **2003**, *37*, 386-391.

(12) Bailey, J. S.; Cosby, D. E. *J. Food Prot.* **2003**, *66*, 2138-2140.

(13) Kapley, A.; Lampel, K.; Purohit, H. J. *Water Environment Research* **2001**, *73*, 461-465.

(14) Warnecke, H.-W. *Fleischwirtschaft* **2001**, *81*, 79-81.

(15) Jenikova, G.; Pazlarova, J.; Demnerova, K. *International Microbiology* **2000**, *3*, 225-229.

(16) Mocuta, N. *World Congress Foodborne Infections and Intoxications, 4th, Berlin, June 7-12, 1998* **1998**, *2*, 830-836.

(17) Podola, B.; Melkonian, M. *J. Appl. Psychol.* **2003**, *15*, 415-424.

(18) Konig, A.; Riedel, K.; Metzger, J. W. *Biosens. Bioelectron.* **1998**, *13*, 869-874.

(19) Endo, G.; Yamagata, T.; Narita, M.; Huang, C. C. *Acta Biotechnologica* **2003**, *23*, 123-129.

(20) Castillo, M.; Barcelo, D. *Tech. Instrum. Anal. Chem.* **2000**, *21*, 537-583.

(21) Bertocchi, P.; Ciranni, E.; Compagnone, D.; Magearu, V.; Palleschi, G.; Pirvutoiu, S.; Valvo, L. *J. Pharm. Biomed. Anal.* **1999**, *20*, 263-269.

(22) Tkac, J.; Gemeiner, P.; Sturdik, E. *Biotechnol. Tech.* **1999**, *13*, 931-936.

(23) Rogers, K. R.; Cao, C. J.; Valdes, J. J.; Eldefrawi, A. T.; Eldefrawi, M. E. *Fundam. Appl. Toxicol.* **1991**, *16*, 810-820.

(24) Kim, N.; Park, I.-S. *Biosen. Bioelectron.* **2003**, *18*, 1101-1107.

(25) Ali, Z.; O'Hare, W. T.; Theaker, B. J. *J. Therm. Anal. Calor.* **2003**, *71*, 155-161.

(26) Kasai, N.; Sugimoto, I.; Nakamura, M. *Chemical Sensors, Technical Digest of the International Meeting, 7th, Beijing, China, July 27-30, 1998* **1998**, 160-162.

(27) Su, X.; Chew, F. T.; Li, S. F. Y. *Anal. Sci.* **2000**, *16*, 107-114.

(28) Yao, S.-Z.; Chen, P.; Wei, W.-Z. *Food Chem.* **1999**, *67*, 311-316.

(29) Malitesta, C.; Valli, L.; Rella, R. *Sensors for Environmental Control, Proceedings of the International Workshop on New Developments on Sensors for Environmental Control, Lecce, Italy, May 27-29, 2002* **2003**, 203-207.

(30) Nanto, H.; Hamaguchi, Y.; Sanada, S.; Nobuyama, K.; Matsumoto, T.; Tanabe, K.; Kurosawa, S. *Chemical Sensors* **2001**, *17*, 363-365.

(31) Syritski, V.; Reut, J.; Opik, A.; Idla, K. *Synthetic Metals* **1999**, *102*, 1326-1327.

(32) Pei, R.; Hu, J.; Zeng, Y. *Huaxue Chuanganqi* **1998**, *18*, 41-48.

(33) Rogers, K. R.; Poziomek, E. J.; Yu, M. *Field Screening Methods for Hazardous Wastes and Toxic Chemicals, Proceedings of an International Symposium, Las Vegas, Nev., Feb. 22-24, 1995* **1995**, *2*, 999-1006.

(34) Chang, S. M.; Kim, Y. H.; Kim, J. M.; Chang, Y. K.; Kim, J. D. *Molecular Crystals and Liquid Crystals Science and Technology, Section A: Molecular Crystals and Liquid Crystals* **1995**, *267*, 405-410.

(35) Wong, Y. Y.; Ng, S. P.; Ng, M. H.; Si, S. H.; Yao, S. Z.; Fung, Y. S. *Biosens. Bioelectron.* **2002**, *17*, 676-684.

(36) Olsen, E. V.; Pathirana, S. T.; Samoylov, A. M.; Barbaree, J. M.; Chin, B. A.; Neely, W. C.; Vodyanoy, V. *J. Microbiol. Methods* **2003**, *53*, 273-285.

(37) Kim, G.-H.; Rand, A. G.; Letcher, S. V. *Biosens. Bioelectron.* **2003**, *18*, 91-99.

(38) Wong, Y. Y.; Ng, S. P.; Ng, M. H.; Si, S. H.; Yao, S. Z.; Fung, Y. S. *Biosens. Bioelectron.* **2002**, *17*, 676-684.

(39) Fung, Y. S.; Wong, Y. Y. *Anal. Chem.* **2001**, *73*, 5302-5309.

(40) Zhang, J.; Wei, W.; Zhou, A.; He, D.; Yao, S.; Xie, Q. *Talanta* **2001**, *54*, 999-1006.

(41) Su, X.; Low, S.; Kwang, J.; Chew, V. H. T.; Li, S. F. Y. *Sensors and Actuators, B: Chemical* **2001**, *B75*, 29-35.

(42) Park, I.-S.; Kim, W.-Y.; Kim, N. *Biosens. Bioelectron.* **2000**, *15*, 167-172.

(43) Pathirana, S. T.; Barbaree, J.; Chin, B. A.; Hartell, M. G.; Neely, W. C.; Vodyanoy, V. *Biosens. Bioelectron.* **2000**, *15*, 135-141.

(44) Park, I.-S.; Kim, N. *Biosens. Bioelectron.* **1998**, *13*, 1091-1097.

(45) Ye, J.; Letcher, S. V.; Rand, A. G. *J. Food Sci.* **1997**, *62*, 1067-1071, 1086.

(46) Goss, C. A.; Charych, D. H.; Majda, M. *Anal. Chem.* **1991**, *63*, 85-88.

(47) Wolfe, C. A.; Hage, D. S. *Anal. Biochem.* **1995**, *231*, 123-130.

(48) Patel, N.; Davies, M. C.; Hartshorne, M.; Heaton, R. J.; Roberts, C. J.; Tendler, S. J. B.; Williams, P. M. *Langmuir* **1997**, *13*, 6485-6490.

(49) Qian, X.; Metallo, S. J.; Choi, I. S.; Wu, H.; Liang, M. N.; Whitesides, G. M. *Anal. Chem.* **2002**, *74*, 1805-1810.

(50) Dong, Y. Doctoral Dissertation, Auburn Univ., Auburn, AL, USA., 2001.